Development and Evaluation of Methodology for Assessing Female Knee-Thigh-Hip Injury Risk in Frontal Impacts Using Female ATD Load Cell Measurements

Randolff L. Carpenter, John-Paul Donlon, Jason L. Forman

Abstract Knee-Thigh-Hip (KTH) injuries are one of the injury types targeted in some frontal-impact vehicle safety assessments. These injuries are sensitive to impact characteristics: lower rate, long-duration knee loading is more conducive to hip injuries, while higher rate, short-duration loading is more conducive to knee/distal femur injuries. Updated knee-thigh-hip injury assessment methods for the Hybrid III midsize male reflect this, incorporating impulse to account for duration dependence and multiple injury risk functions to reflect differences in force tolerance. Despite this, many KTH assessment methods still use older approaches, such as FMVSS 208, which only assesses knee/distal femur injury risk. Furthermore, efforts to adapt the updated methodology for THOR-50M have raised concerns about representativeness. This is important, as similar methods for small female ATDs are either absent or scaled from male assessments. This study used experimental data and analytical models of female cadavers and ATDs to investigate methods for relating ATD load cell forces to KTH injury risk in female occupants. Results suggest that incorporating impulse provides a more comprehensive assessment than using peak force alone. Further, this approach produced the most consistent injury risk distribution estimates across ATDs, providing confidence as more ATDs are introduced into standardized assessments.

Keywords ATDs, Female, Injury Assessment, Knee-Thigh-Hip, Lumped-Parameter Modelling.

I. INTRODUCTION

Although less fatal than other injury types, Knee-Thigh-Hip (KTH) injuries are among the affected body regions in frontal collisions and can significantly impact an individual's quality of life [1-3]. These injuries are thought to occur when an occupant interacts with the lower instrument panel, knee airbag, or seatbacks during a frontal collision, loading the anterior surface of the flexed knee [1,2,4-8]. The force is then transferred along the femur to the hip, with injuries possible at any point along this path. However, the force transfer along KTH is only a fraction of the initial force applied to the knee due to the acceleration of the increasingly recruited mass along the KTH load path. It is currently not feasible to measure these forces directly in post-mortem human subjects (PMHS, cadavers) without disturbing the mass coupling behaviour [4,7-9].

This limitation affects KTH research and vehicle design by hindering accurate and consistent injury assessment methods. Predictive tools, such as Anthropomorphic Test Devices (ATDs), are used to predict human responses and assess injury risk. ATDs aim to replicate the internal and external loading conditions that a human would experience. However, the stiffer construction of ATDs can interfere with capturing accurate human-like responses due to differences in external and internal biofidelity. Correction factors are often applied to translate ATD measurements into cadaver-based injury risk functions (IRFs). However, these values require an understanding of the underlying assumptions and their applicability. Due to biofidelity differences, no single correction factor can encompass every impact scenario [8]. Therefore, KTH injury assessments require tuning to balance sensitivity (accurately identifying impacts that would exceed a specified injury risk threshold) and specificity (accurately identifying impacts that would not exceed a specified injury risk threshold). The optimal method should robustly identify both the presence and absence of KTH injury across the maximum number of cases, maximizing both sensitivity and specificity. This becomes further complicated as the approaches currently used can produce vastly different assessments of KTH injury, potentially leading to mixed usage and inconsistencies in the literature [1,8,10-12]. Without a consistent KTH injury assessment method, efforts to develop countermeasures may be ineffective or expose other body regions to higher injury risks.

Past literature on KTH injury assessment methods for midsize male ATDs relied on correction factors from experimental testing or a combination of experimental and analytical methods [1,8,10,11,13-15]. Early KTH IRFs were developed based on knee impacts that showed a large prevalence of knee and distal femur injury with very few hip injuries. Consequently, the knee and femur were considered to have the lowest force tolerance of KTH, and protecting the femur became the primary focus [16-21]. When the Hybrid III midsize male ATD was tested under similar conditions, the force recorded in the Hybrid III femur load cell was approximately equal to the knee impact force at the PMHS knees [22,23]. As a result, no correction factor was used, allowing direct application of the Hybrid III femur load cell to the original KTH IRF. For regulatory testing, a maximum-force injury criterion of

R. L. Carpenter is a PhD student (phone: 434-297-8009, email: rlc4gj@virginia.edu), P. R. Berthelson is a Mechanical Engineer, J. P. Donlon is a Senior Research Specialist, and J. L. Forman is a Principal Scientist at the University of Virginia's Center for Applied Biomechanics in Charlottesville, Virginia.

10 kN for axial femur loading was established in the Hybrid III, associated with a 35% risk of AIS 2+ injury to the KTH complex [11,22]. This criterion was then scaled to 6.805 kN for the small female Hybrid III, both of which are still prescribed in FMVSS 208 [24,25].

Real-world crash data suggests that KTH injuries are often comprised of a mix of knee, femur and hip injuries [5,26]. Follow-up PMHS component studies found the hip, specifically the posterior acetabulum, as the weakest component in the KTH loading pathway in terms of force tolerance, and led to the development of a hip IRF for use in frontal impact crash testing [5,14,15,27]. The inconsistency with the test results discussed above (where the injuries were predominantly in the knee/distal femur) was attributed to the choice of impactors used in previous test series, which were rigid or lightly padded, resulting in high knee and distal femur injury rates but few hip injuries [11-16]. In contrast, the updated test series used energy-absorbing padding materials to reduce these injuries by increasing loading duration and lowering loading rates, which are more likely to cause to hip injuries [7,14,15,27-30]. Validation tests also showed that the updated impactor material was more representative of regulatory crash conditions [7].

The updated KTH tolerance tests helped clarify the higher prevalence of hip injuries in crash data. However, the lack of KTH force transfer knowledge for midsize males and the relationship between KTH force transfer in midsize males and ATDs made it unfeasible to directly apply this understanding to ATDs, as the hip IRF required cadaver hip force, which was unknown. To apply ATD load cell measurements to cadaver-based IRFs through a correction factor, the KTH force transfer in midsize male cadavers and the Hybrid III ATD was defined using combined experimental and analytical approaches [7,8]. By hierarchically removing mass, changes in loading and kinematic behaviour across impact conditions were attributed to springs and dampers in an analytical model. Developing the model in reverse hierarchical order from experimental tests allowed prediction of KTH force transfer in whole-body conditions for both the PMHS and ATDs. Correction factors were derived to express midsize male PMHS KTH forces in terms of the Hybrid III femur load cell force by exciting the analytical models over various impact conditions and comparing KTH force transmission across subjects. This was then used to develop a more robust methodology for estimating human KTH injury risk from ATD load cell measurements. To account for differences in KTH injury tolerance as a function of loading duration, impulse was used as an additional metric. This methodology was then validated in a follow up study by [31], and has since been adapted by the Insurance Institute for Highway Safety (IIHS) to evaluate vehicle crashworthiness [32].

While those methods advance our understanding of KTH injuries, their representativeness for a diverse population remains unproven. Specifically, recent investigations have observed significant differences in lower extremity injury risk between females and males [33-35]. This trend suggests a need to revisit the assumptions used to estimate KTH force transfer characteristics and injury tolerance for females via scaling from midsize male datasets [8,10]. This study aimed to develop and compare methods for assessing KTH injuries using load cell measurements from small female ATDs, following similar assumptions from past literature [1,8,10], but using female-specific ATD and PMHS data from [36,37]. To explore the suitability of each method, various sources were used, including non-injurious bilateral knee impact tests [36,37], analytical simulation data, and NCAP passenger data from 2010-2023 model year (MY) vehicles.

II. METHODS

Experimental Tests Used for Model Development

Experimental testing involved the use of the Hybrid III and THOR 5th percentile female ATDs, as well as four female PMHS, which have been previously reported by [36,37] and will only be summarized here. To simulate a frontal KTH impact, PMHS were seated upright and struck in the knees by a ram coupled to a pneumatically driven linear actuator with active feedback. Each knee was impacted by a six-axis load cell covered by Sorbothane padding. The seat and footpan were lined with low-friction material and mounted on six-axis load cells to measure subject interaction. PMHS were tested at velocities of 2.5, 3.5, 4.9, and 7.2 m/s, chosen based on previous impact data to assess responses across a range of frequencies [7].

Tests followed a hierarchical procedure: Whole Body (WB) condition at 2.5, 3.5, and 4.9 m/s; Thigh Flesh Removed (TFR) condition at 3.5 m/s; Thigh Flesh Removed plus Load Cell (TFR+LC) condition at 2.5, 3.5, and 4.9 m/s; and Torso Removed (ToR) condition at 3.5, 4.9, and 7.2 m/s. Individual segment masses were recorded for developing subject-specific lumped parameter models. Similar experimental tests for small female ATDs were conducted in the WB condition at 2.5, 3.5, and 4.9 m/s, but damage limited further testing [36]. The presence of load cells, definable mass segments, and rigid mass coupling, along with previous values for midsize male ATDs

[8,28], provided sufficient information to establish analytical model parameters for the ATDs.

Development of a Generalized Small Female Model

To derive the injury assessment methods, a generalized small female analytical model was necessary, as only subject-specific investigations had been conducted previously. Its development followed a similar procedure to that used for subject-specific female LPMs, as reported by [37]. The model structure, shown in Fig. A1, uses an eight degree-of-freedom mass-spring-damper system represented by a series of second-order differential equations. Each mass for the generalized model was derived from the average of the individual segment masses recorded during autopsy from the original tests. The subjects in the original study ranged from 45.4 to 59.0 kg, with an average mass of 51.3 ± 5.7 kg. Since the analytical models used are mass-based, deriving a generalized small female LPM from the previously established subject-specific models is reasonable, as the mass of a typical small female and the current small female ATDs are within these bounds [36,38].

To obtain the spring and damper values, a three-part optimization was conducted in reverse hierarchical order of the experimental testing, using the average kinematic and loading behaviour across subjects. The upper and lower optimization bounds for each spring and damper in the generalized model were selected to ensure the tuned values fell within the range of the final subject-specific values. A pattern search optimization was used, followed by multiple surrogate optimizations to limit the likelihood of the final solution representing a local minimum. Once the whole-body model was finished, force transfer along KTH could be determined. The final values are detailed in Appendix A, along with plots of the WB model predicted forces and kinematics (Fig. A2-A8). The ratio of the model-predicted hip force relative to the maximum applied knee force was 55±2%, aligning with the predicted value from averaging the subject-specific female analytical models in [37].

Development of a THOR-05F Model

To obtain the model masses described in Fig. A1 for THOR-05F, the ATD, including its jacket and footwear, was disassembled to measure the segment masses. Since only whole-body tests were available for optimization, a single optimization was performed to tune the stiffness and damping interactions between the masses. This optimization minimized the normalized area between the measured and predicted femur and hip forces in the models for 2.5 and 3.5 m/s impacts. The 4.9 m/s test, not part of the optimization, was used to validate the final values. Additionally, the time to peak force, peak forces, and impulse of loading were compared to ensure minimal error in the model's predicted values.

The final values for the THOR-05F model optimization are reported in Table B1, along with validation figures (Fig. B1-B3) and the final error between the femur and hip loading characteristics (Table B2-B3). The validation results show minimal differences between the model-predicted values and the measurements recorded from the femur and acetabular load cells during testing. Specifically, there was no difference in femur load cell force transmission from the knee (83% predicted vs. 83% measured), and in force transmission from the knee to the acetabular load cell (41% predicted vs. 41% measured).

Simulations to Investigate Relationship Between Peak Forces in the ATD Load Cells and Peak Force at the PMHS Hip

Although force transfer relationships can be determined through experimental testing, they only represent a subset of knee impact conditions in frontal collisions. ATDs and PMHS exhibit different KTH force transfer relationships during knee impacts due to inherent differences in stiffness and mass coupling among subjects, which are further exacerbated by variations in the contact material [8,36]. This is significant because production vehicles utilize knee bolsters with varying force-deflection characteristics, leading to greater diversity across vehicles as researchers seek new ways to manage impact forces applied to the knee and minimize the risk of KTH injury. Thus, it is essential to quantify the variability in force transfer among different subjects under a wide array of impact scenarios and leverage the data to develop and validate a comprehensive injury assessment framework. Achieving this solely through experimental approaches would require an impractical number of matched knee impact tests. Instead, a modelling approach is more feasible and can be adapted from methods previously established for midsize males [8], allowing for continuity.

To model differences in impact conditions across production knee bolster designs, the original study categorized the force-deflection profiles for each knee bolster into three generalized forms [8]. The first form is a simple linear bolster, where the force increases linearly as the knees penetrate the bolster (Fig. 1A). The second is a more complex spring with a bilinear profile, consisting of two different stiffness regions and a transition force (Fig. 1B). The third form is a force-limiting spring, where the force increases linearly with deformation up to a specified force limit and then remains at that limit despite further bolster penetration (Fig. 1C). As illustrated in the figures, varying the stiffness profiles can produce different applied knee forces for similar impact severities, stemming from differences in subject knee bolster penetration. This variation further complicates the ability to relate the ATD load cell forces to the forces experienced along the KTH complex of a female cadaver, as there is not singular relationship applicable to all impact scenarios [8].

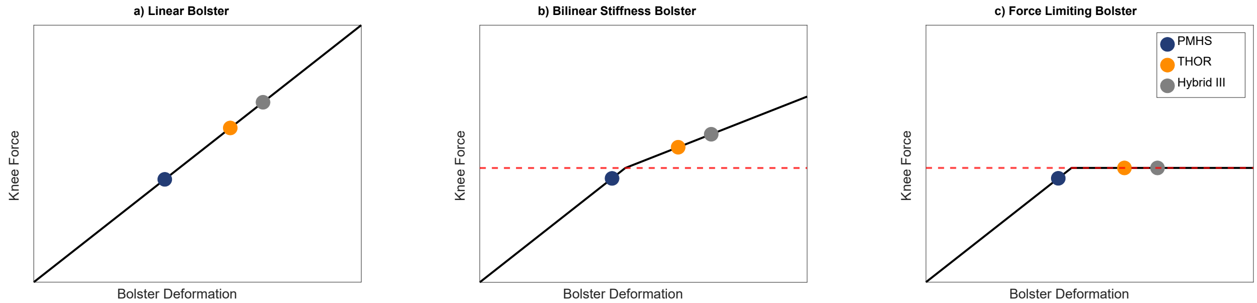

Fig. 1. Generalized forms of production knee bolsters, adapted from [8].

To incorporate these bolster profiles into the analytical model, a new mass term, *mI*, representing the mass of the impactor, was connected to the knee/distal femur (mA) by a spring element, *kIA*, representing the knee bolster stiffness profile (Fig. C1). To model the impact velocity, an initial velocity was prescribed for the impactor mass (*mI*), with the remaining subject masses initially at rest. Using the small female generalized and ATD models along with the knee bolster stiffness parameters, a full factorial of simulations was performed, producing a matched pair dataset between subjects (Table C1). These parameters were selected to remain consistent with the methods of [8], representing impacts characteristic of more severe US NCAP and FMVSS 208 tests on 1998-2004 MY vehicles, up to rigid non-bolster-like loading. The simulations output the loading characteristics along KTH and subject penetration into the bolster (Appendix C). These results were used to define KTH force transfer relationships and assess the feasibility of KTH injury risk assessment methods developed in the following sections.

Knee/Distal Femur and Hip Injury Risk Function Selection

To evaluate the risk of knee/distal femur injuries for small female ATDs and PMHS, the recommended risk function for THOR-50M to predict AIS 2+ knee/femur injury was used [1], assuming a female (♂=0), yielding Eq. 1:

$$p(Knee/Distal\ Femur\ AIS\ 2+) = \Phi\left[\frac{Ln\left[F_{\max_{Knee}}\right] - 2.224}{0.3014}\right] \quad (1)$$

where Φ is the cumulative normal distribution function and $F_{\max_{Knee}}$ is the maximum force applied to the female PMHS knees during the impact. This IRF is based on a re-evaluation of data considering covariates such as sex, stature, age, and mass using logistic regression and survival analysis [29]. The original dataset came from tests on cadavers where force was applied to the knee and the presence of AIS 2+ injury to the femur or knee was assessed [11]. In the updated analysis, sex significantly affected the prediction of knee/femur injury risk, so it is included as a covariate in the final risk function. While age and mass were considered, mass was not a significant predictor, and age, though statistically significant, was not included due to large confidence intervals. Stature was also not added, likely due to its strong correlation with sex in the dataset.

To evaluate the risk of hip injuries for the small female ATDs and PMHS, the recommended risk function for THOR-50M to predict hip fracture was used, as reported in [1], along with common assumptions for a small female (stature = 150 cm, hip flexion angle = 15°) [14,29], yielding Eq. 2:

$$p(Hip\ FX) = \Phi\left[\frac{Ln\left[F_{\max_{hip}}\right] - 1.309}{0.2339}\right] \quad (2)$$

where Φ is the cumulative normal distribution function and $F_{\max_{hip}}$ is the maximum hip force recorded in kilonewtons. Hip fracture has been previously defined by [1,29] as a fracture of the acetabulum, pubic rami, femoral head/neck, and/or hip dislocation. The resulting hip injury can be coded as either AIS 2 or 3 depending on the severity of the fracture, as established by [39]. Eq. 2 is based on a reanalysis of the data originally reported in [29], which used stature, hip flexion angle, and hip abduction angle as covariates. In the follow up analysis reported in [1], only stature and flexion angle were found to be significant components of the function, and abduction angle was excluded to limit the number of variables. To examine the 15° flexion angle assumption, [1] compared previous frontal sled tests, showing that the hip flexion angles at the time of peak femur load were approximately 15° across subjects, suggesting this estimate is reasonable.

Using these IRFs, KTH IARVs can be established for the small female, as shown in Appendix D. These values depend on the assumptions used to define the IRFs and are separate from the current experimental and analytical approach. The findings of this study will be applied to these values by incorporating ATD correction factors, discussed in the next section.

Selection of Correction Factors for ATD Load Cell Measurements

To express the IRFs in terms of ATD load cell measurements, correction factors based on the KTH force transfer relationship between ATDs and female PMHS are often required. The ATD-to-PMHS knee correction factor, T_{knee}, has been previously established for the Hybrid III midsize male femur load cell [8] and THOR-50M femur and acetabular load cells [1], defined as (Eq. 3):

$$\mathrm{T_{Knee}} = \begin{cases} \dfrac{1}{r_{KH_{THOR}}} & \text{for THOR acetabular load cell} \\ \dfrac{1}{r_{KT_{THOR}}} & \text{for THOR femur load cell} \\ \dfrac{1}{r_{KT_{H3}}} & \text{for Hybrid III femur load cell} \end{cases} \tag{3}$$

where T_{Knee} is the ratio of the PMHS impact force relative to the force transmission to the Hybrid III femur load cell ($r_{KT_{H3}}$), THOR femur load cell ($r_{KT_{THOR}}$), or THOR acetabular load cell ($r_{KH_{THOR}}$). Similarly, the correction factor (T_{hip}) for expressing the cadaver-derived hip IRF from Eq. 2 in terms of ATD load cell measurements, has been established for the midsize male ATDs [1,8], defined as (Eq. 4):

$$T_{Hip} = \begin{cases} \dfrac{r_{KH_{PMHS}}}{r_{KH_{THOR}}} & \text{for THOR acetabular load cell} \\ \dfrac{r_{KH_{PMHS}}}{r_{KT_{THOR}}} & \text{for THOR femur load cell} \\ \dfrac{r_{KH_{PMHS}}}{r_{KT_{H3}}} & \text{for Hybrid III femur load cell} \end{cases} \tag{4}$$

where T_{hip} is the ratio of estimated PMHS hip force to Hybrid III measured peak axial femur force and THOR measured peak acetabulum resultant force, $r_{KH_{PMHS}}$ is the ratio of applied force at knee to hip force obtained from the results of the generalized female model, and the remaining variables were defined above. These values are then applied to their respective IRFs by substituting the maximum force term (F_{max}) with the product of the maximum load cell measurement recorded and the correction factor ($T_{Knee\ or\ Hip} * F_{LC_{max}}$).

These correction factors have been designed around two primary scenarios [1,8,10,11]. The first scenario relies on the average experimentally observed KTH force transfer relationship. For the Hybrid III ATD, after replicating knee impacts that produced KTH injury in cadavers, the force recorded in the Hybrid III femur load cell was similar to the impact force at the cadaver knee [23]. Thus, a correction factor was not necessary ($T_{Knee} = 1$), and the original cadaver-based KTH IRF was used directly with the peak force recorded in the Hybrid III femur load cell [10,11]. However, this approach does not cover all ATD load cell combinations resulting in injury due to the inherently lower sensitivity from assuming average conditions. Therefore, as impact conditions deviate and the force transfer relationship changes from the experimental case, the effectiveness of this method decreases.

To provide a more robust assessment of KTH injury across variations in knee-bolster designs, recent work recommends considering a broader range of knee impact cases, thus designing methods around a conservative impact scenario [1,8,28]. This scenario occurs when peak applied knee forces are equal among subjects, representing the lowest ATD forces associated with a specified risk of KTH injury in human subjects, only achievable using a force-limiting knee bolster [8,28]. The reasoning is that the relative stiffness of the ATDs inhibits the impact force from being lower than that of the PMHS under matched conditions, due to differences in bolster penetration among subjects [1,4,8]. This approach, by definition, produces injury risk estimates with nearly 100% sensitivity, which is much higher than previous scenario [1,8,28]. It also implies that results interpreted directly from the IRFs are more likely to provide an unrealistic representation of a human under similar conditions due to the over predictive nature of the method.

Development of Force-Impulse Assessment Boundaries for Small Female ATDs

Direct application of the correction factors to the IRFs is further complicated by the fact that hip injuries typically occur in lower-rate, longer-duration knee loading conditions, whereas knee/distal femur injuries are more likely to occur in higher-rate, shorter-duration impacts [8]. Force-based IRFs alone cannot differentiate between these mechanisms, limiting their specificity [8]. This limitation has been explored through the KTH Injury Assessment Reference Boundary (IARB) method, which balances the conservative estimates provided by the second impact scenario, with loading duration [8]. This method theoretically achieves nearly 100% sensitivity with greater specificity compared to using force-based methods alone. Each IARB is defined by three key components: the lower-force limit, the transition impulse, and the upper-force limit (Fig. 2). The lower force limit represents the minimum ATD load cell force associated with a specified risk of hip injury in a human subject. If the peak load cell force recorded in the ATD exceeds this limit, a hip injury may be possible for the specified risk level. The upper force limit represents the corresponding risk of knee/distal femur injury, which is higher when applied to the same load cell since hip force tolerance is lower. If the peak force exceeds this limit, both knee/distal femur and hip injury risks are greater than the specified risk level.

If the peak load cell measurement falls between the upper and lower force limit boundaries, only a hip injury would be predicted if the measurement exceeds the lower force limit but not the upper force limit. In some scenarios, impacts in this region would not realistically produce hip injuries due to insufficient loading duration [8]. To account for this, a transition impulse is added that bridges these two limits, increasing specificity to account for the heightened sensitivity. This value is defined as the integral from the time when the load cell enters compression to the time when the force last falls below the transition force, representative of the minimum force associated with injury in the original hip tolerance tests [8].

Using this method, small female IARBs were developed for the Hybrid III femur load cell, corresponding to various levels of KTH injury risk consistent with previous research [8]. For THOR, which has load cells in both the femur and acetabulum, separate KTH IARBs were developed for each location. The lower limit for each ATD load cell was derived by substituting $T_{Hip} * F_{LC_{max}}$ for $F_{\max_{Hip}}$ in Eq. 2, where T_{Hip} is a unique correction factor for each ATD load cell location derived from Eq. 4. The upper force limit was derived by substituting $T_{knee} * F_{LC_{max}}$ for $F_{\max_{Knee}}$ in Eq. 1, where T_{Knee} is a unique correction factor for each of the relationships shown in Eq. 3.

To determine the upper bound of integration for the transition impulse, the 2.89 kN value from the original study was scaled using methods for translating forces from midsize males to small females [40]. This scaling yields a lowest hip fracture force for the small female of 2.28 kN, calculated as 2.89 kN [8] times a force scale factor of 0.79 [40]. This value was verified by comparing it to the Hip IARVs derived using Eq. 2 to ensure the upper bound of integration was below all risk levels. Applying the inverse of the correction factor T_{Hip} from the conservative impact assumption, transition impulses were determined from the start of loading to the transition force (Fig. 3). This force is consistent across different risk levels but unique for each ATD load cell. Transition impulses were then calculated for each risk level by simulating the analytical models to find the minimum impulse in the ATD load cells associated with a risk of hip injury greater than or equal to the specified risk in the PMHS. This was achieved using a 450 N/mm stiffness force-limiting bolster, which results in the highest knee loading rate and the shortest duration of applied force for the conservative approach [8].

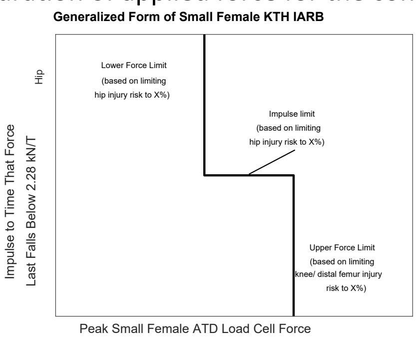

Fig. 2. Generalized form of small female ATD KTH IARB, adapted from [8].

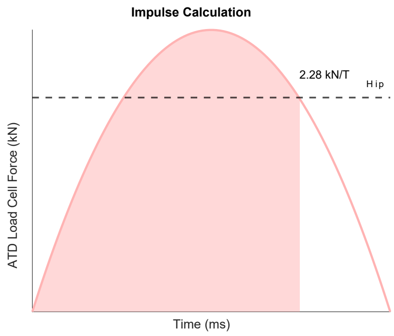

Fig. 3. Generalized small female ATD impulse calculation, adapted from [8].

Evaluation of KTH Injury Risk Assessment Methods

After developing the small female KTH injury assessment methods, they were evaluated using small female ATD KTH impact responses from various sources to determine their effectiveness in producing reasonable injury assessments. The three methods included both the experimental and conservative correction factors applied directly to the IRFs, and the KTH IARBs. The evaluation sources included ATD load cell measurements from experimental knee impact tests [36], model-estimated load cell measurements obtained from the analytical simulations, and Hybrid III load cell measurements from NHTSA NCAP and vehicle research tests conducted using 2010-2023 MY vehicles. Across all sources, it was assumed that changing either the measurement location (femur or acetabulum) or ATD model should not drastically affect the KTH injury risk assessment.

For the experimental knee impact tests, the female cadavers did not sustain KTH injuries under the 2.5, 3.5, and 4.9 m/s whole-body impact conditions [36,37]. Therefore, any method predicting a high risk of KTH injury in these scenarios would be unrealistic. In contrast, the analytical simulations were designed to encompass a broad spectrum of impact conditions, ranging from those observed in US NCAP and FMVSS 208 tests on older vehicles to scenarios involving rigid, non-bolster-like knee loading [8]. Consequently, the injury risk distribution across all simulations should reflect a higher likelihood of KTH injury. Finally, newer NCAP and vehicle research tests were incorporated to evaluate behaviour under impacts representative of modern vehicles, and in belted occupants which were not targeted in the previous data sources. These evaluations should yield lower KTH injury risk estimates due to two key factors: 1) advancements in vehicle safety since the 1998-2004 MY vehicles used to define the analytical simulation parameters [33,34], and 2) the inclusion of seat belts, which have been shown to limit forward knee excursion and reduce overall KTH injury risk compared to unbelted occupants [31].

To enable a direct numerical comparison across injury assessment methods and contextualize the predictions relative to human injury risk data, all ATD-based injury risk methodologies were converted into continuous IRF formats. This required translating the discrete IARBs into continuous risk curves, consistent with the approach used in previous evaluations of the Hybrid III midsize male and scaled small female ATD IARBs [31]. For force-based injury predictions, the base IRFs defined in Equations 1 and 2 were used. These functions were applied to peak femur or acetabular forces recorded from the ATD load cells, with the appropriate correction factors applied for each assessment approach. To convert the transition impulse thresholds in the IARBs into continuous risk functions, a logistic risk model was fitted to the set of subject-specific transition impulse values (Eq. 5):

$$p_{hip,impulse} = \frac{a}{1+\left(\frac{impulse}{b}\right)^{-c}} \tag{5}$$

where a, b, and c are parameters determined through nonlinear curve fitting. For the IARB-based method, the predicted hip injury risk for each measurement point was calculated as the minimum of the force-based and impulse-based predictions [8,31], expressed as (Eq. 6):

$$p_{hip} = min\left(p_{hip,force}, p_{hip,impulse}\right) \tag{6}$$

Overall KTH injury risk was then calculated as (Eq. 7):

$$p_{KTH} = max\left(min\left(p_{hip,force}, p_{hip,impulse}\right), p_{knee}\right) \tag{7}$$

For force-based methods, the impulse term was excluded, and hip injury risk was determined directly from the force-based IRF. For the analytical simulations, injury assessment methods were evaluated using the coefficient of determination (R^2), root mean squared error (RMSE), and bias. R^2 quantified correlation between ATD- and PMHS-predicted injury risks, RMSE measured average prediction error, and bias indicated whether methods overpredicted (positive) or underpredicted (negative) PMHS responses. For experimental knee-impact tests, the PMHS-predicted injury risk was compared with the average injury risk estimate from each assessment method for each impact velocity tested. In the U.S. NCAP dataset, where direct PMHS data were unavailable, predicted KTH injury risks were assessed relative to field injury trends, using the dataset from [41].

III. **RESULTS**

Correction Factor Estimates from Force Transfer Relationships

The ATD-to-PMHS correction factors, shown in Table 1, are based on different impact scenarios. The average experimental results represent correction factors derived from force transfer data in [36], relative to the applied PMHS knee force. This approach follows traditional assumptions for expressing cadaver-based IRFs using ATD load cell measurements [10,23]. For the Hybrid III ATD, the femur load cell force transmission averaged 109% of the PMHS knee force. For the THOR ATD, the femur and acetabular force transmission averaged 103% and 52% of the PMHS knee force, respectively. Using these values in Eq. 3, the ATD-to-PMHS knee force correction factors (T_{Knee}) are 0.92, 0.97, and 1.92 for the Hybrid III femur load cell, and the THOR femur and acetabular load cells, respectively. This indicates that the ATD femur load cell peak values closely matched the PMHS knee force, while the THOR acetabular force was about half of the PMHS knee force. Considering the experimental knee-to-hip force transmission for the small female model, which estimated 55% transmission, the same ATD load cell values were applied to Eq. 4 to obtain the ATD-to-PMHS hip force correction factors (T_{Hip}). The resulting values are 0.50, 0.53, and 1.06 for the respective load cells, indicating that the ATD femur load cells were approximately double the PMHS hip force, while the THOR acetabular load cell was similar in magnitude.

The second set of correction factors was derived from the average simulation-predicted KTH force transmission for each subject. This was achieved by normalizing the force transmission by dividing the peak force at the femur and hip by the corresponding peak force applied at the knee, separate from the previous assumption that normalized all values relative to the peak PMHS knee force. These factors follow recent assumptions used for KTH injury assessment, representing a direct relationship between the peak force at the ATD load cells and the peak force at the cadaver hip when both load the knee bolster to its force limit, using a force-liming bolster [1,8]. The percentage of force transmitted from the initial impact force to the femur load cell averaged 80% for the Hybrid III ATD and 81% for the THOR ATD across all simulations. Force transmission to the acetabular load cell from the knee averaged 40% for the THOR ATD. For the generalized PMHS model, the force transmission from the knee to the hip averaged 56% across all simulations. These values were relatively constant over the simulation parameters explored, indicating that, independent of variations in knee bolster stiffness profiles, the ratio between the ATD load cell force transmission and PMHS knee force can be expressed as 1.25 (1/0.80), 1.23 (1/0.81), and 2.50 (1/0.40), corresponding to T_{Knee} for each of the respective load cells (Eq. 3). Similarly, applying Eq. 4 yields values of 0.70 (0.56/0.80), 0.69 (0.56/0.81), and 1.40 (0.56/0.40), corresponding to T_{Hip} for each of the respective load cells. Applying both sets of correction factors directly to the IRFs from Eq. 1-2 represents two methods currently used to assess KTH injury in the ATDs [1,10,11].

TABLE I
KTH CORRECTION FACTOR ESTIMATES FOR SMALL FEMALE ATDS

Force Transmission	Subject	Load Cell	$r_{KT_{ATD}}$	$r_{KH_{ATD}}$	$r_{KH_{PMHS}}$	T_{Knee}	T_{Hip}
1. Average Experimental Results [36] (Normalized by PMHS Peak Applied Force)	Hybrid III	Femur	1.09	--	0.55	0.92	0.50
	THOR	Femur	1.03	--	0.55	0.97	0.53
	THOR	Acetabulum	--	0.52	0.55	1.92	1.06
2. Average Simulation Results (Normalized by Each Subject's Peak Applied Force)	Hybrid III	Femur	0.80	--	0.56	1.25	0.70
	THOR	Femur	0.81	--	0.56	1.23	0.69
	THOR	Acetabulum	--	0.40	0.56	2.50	1.40

Derivation of KTH Injury Risk Assessment Boundaries for the Small Female ATDs

To establish KTH IARBs, only the conservative correction factors were used, consistent the previous approach [8]. The lower-force limit for small female ATDs was determined by incorporating the values of T_{Hip} into the Hip IRF (Eq. 2). Transition forces were calculated by multiplying the inverse of the correction factors (T_{Hip}^{-1}) by 2.28 kN (to convert from cadaver to ATD force), resulting in 3.26 kN (2.28/0.70) for the Hybrid III femur load cell, 3.30 kN (2.28/0.69) for the THOR femur load cell, and 1.63 kN (2.28/1.40) for the THOR acetabular load cell. These values define the upper bound for the transition impulse calculation. The upper force limits were determined by incorporating T_{Knee} into the knee/distal femur IRF (Eq. 1). The complete list of IARBs, corresponding to injury risks of 3%, 5%, 10%, 15%, 25%, 30%, 35%, 40%, 45%, 50%, and 75%, is shown in Tables E1-E2, with an example derivation of a 25% risk boundary for each ATD load cell in Appendix F.

To contextualize the final small female IARB values relative to previous work, the Hybrid III results were compared to the values provided in [8,31], obtained via scaling methods (Table E1, Fig. E4-E5). Despite using slightly different hip IRFs, the lower force limits are similar between studies, as both use similar assumptions for a small female. Transition impulse values were also consistent, with minimal differences due to the similarity in Hip IRFs. Lastly, the upper force limits exhibited slight deviations at lower risk levels due to differences in the methods used to adapt these values for a small female.

To assess the overall injury risk distribution estimated by the IARBs, the 5%, 15%, and 25% values were used, as these represent the current values used by IIHS for the Hybrid III midsize male ATD [32] (Fig. 4). Due to the lack of similar IARBs for the THOR-50M, these values were estimated by updating the recommended THOR-50M ATD KTH IRFs in [1] assuming similar ATD correction factors, and scaling the THOR-05F transition impulses using established techniques [8,40]. The detailed derivation is provided in Appendix E. Lastly, to derive the continuous impulse-based IRFs from the discrete transition impulses obtained, the transition impulse thresholds from each subject were fitted to Eq. 5. This fit was performed separately for each ATD load cell. The fitted parameters (a, b, c) are shown in Table E4. For the THOR-50M, impulse risk curves were estimated by scaling the b-parameter from the THOR-05F results by a factor of 1.47, consistent with the methodology in [31].

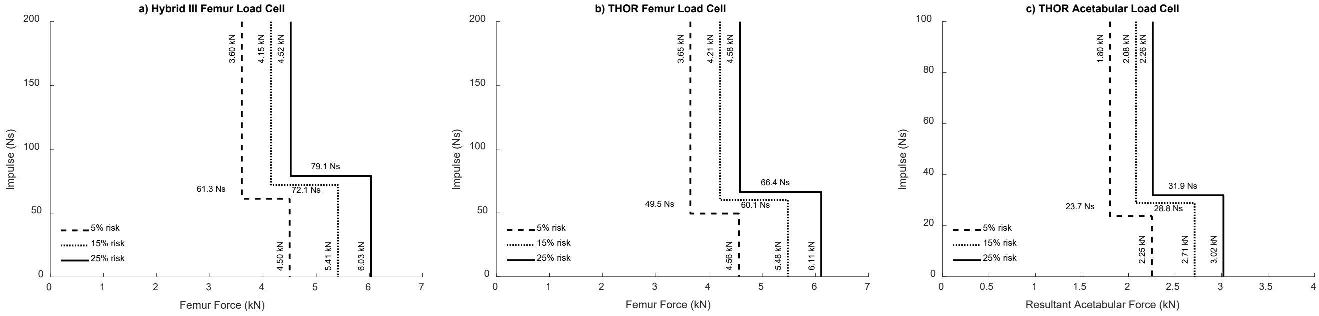

Fig. 4. Injury Assessment Reference Boundaries for each of the small female ATD load cells corresponding to a 5, 15, and 25% risk of KTH injury.

Comparison of KTH Injury Risk Assessment Methods using Simulation Data

The compressive femur force and impulse distribution estimated for each subject and load cell location across the analytical simulations is presented in Fig. 5, with the IARB method applied and other methods shown in Appendix G. The various methods yielded differing injury risk values, generally trending toward higher estimates (>25%), consistent with the severity of the simulated knee impact conditions. Applying experimentally derived correction factors directly to the KTH IRFs resulted in lower injury risk estimates on average compared to other methods. In contrast, the conservative force-only approach produced the highest risk estimates for each subject. Incorporating impulse into the calculation yielded distributions that fell between these extremes.

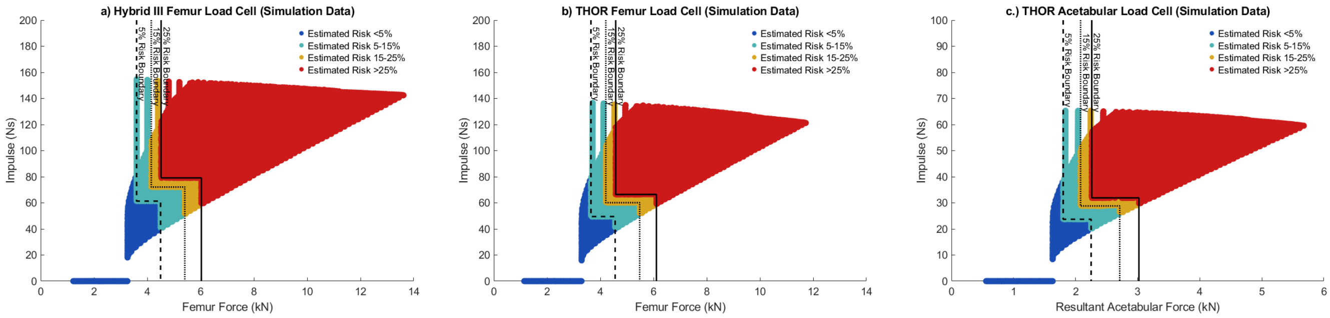

Fig. 5. Distribution of force-impulse responses at each small female ATD load cell location predicted by the analytical simulations. Distributions are categorized by an estimated KTH injury risk <5%, 5-15%, 15-25%, and >25%.

TABLE II
COMPARISON OF ESTIMATED KTH INJURY RISK BY EACH APPROACH ACROSS ANALYTICAL SIMULATION DATA

Assessment Approach	*Subject*	*Load Cell Location*	*R^2*	*RMSE (%)*	*Bias (%)*
IARB (Force + Impulse)	Hybrid III	Femur	0.69	16.6	12.4
		Femur (Scaled) [8,31]	0.59	19.1	14.3
	THOR	Femur	0.77	14.2	9.8
		Acetabulum	0.76	14.6	10.2
Experimental (Force Only)	Hybrid III	Femur	0.65	17.7	-4.6
	THOR	Femur	0.59	19.1	-11.1
		Acetabulum	0.55	19.9	-12.4
Conservative (Force Only)	Hybrid III	Femur	-0.21	32.8	25.1
	THOR	Femur	0.31	24.8	17.6
		Acetabulum	0.33	24.4	17.4

Table 2 summarizes the comparative performance of each approach. For every simulation, PMHS-predicted KTH injury risk was evaluated against predictions derived from Hybrid III and THOR ATD load cells. Assessment performance was quantified using R^2, RMSE, and Bias. Among the evaluated methods, the IARB approach demonstrated the strongest agreement with PMHS-predicted injury risk across all load cell types, particularly for the THOR femur and acetabular load cells. When applying scaled injury risk estimates for the Hybrid III small female proposed by [31], predictive performance declined, with R^2 values decreasing and RMSE and bias increasing relative to current IARB estimates. The experimental force-only approach exhibited a slight underprediction bias and weaker correlation compared to the IARB method. In contrast, the conservative force-only approach tended to substantially overpredict responses and showed poorer overall fit relative to the other methods, particularly for the Hybrid III femur load cell, where the R^2 value was negative.

Inter-subject variability in predicted risk was primarily driven by bolster penetration differences, with Hybrid III exhibiting the highest penetration and THOR falling between PMHS and Hybrid III responses (Table C6). On average, THOR estimated 87% of the Hybrid III knee bolster penetration across all simulations, resulting in reduced sensitivity to changes in bolster stiffness profiles and a narrower distribution of force-impulse responses compared to Hybrid III (Fig. 5). Additionally, within the THOR ATD, results for all approaches were generally consistent between the femur and acetabular load cells, with minor differences likely stemming from the compliant element separating the measurement locations.

Comparison of KTH Injury Risk Assessment Methods using Knee Impact Tests

The compressive femur force and impulse distributions measured in the experimental knee impact tests [36] is shown in Fig. 6, with the IARB method applied and additional approaches detailed in Appendix G. Injury risk estimates were generally low (<25%), consistent with prior PMHS knee impact tests [37], which reported an absence of KTH injuries under similar conditions. Further, all impacts were below the 6.805 kN IARV prescribed in FMVSS 208 (Fig. 6A). For the Hybrid III femur load cell, there was larger variability in peak femur force observed during the highest impact velocity. Since only one impact test was conducted using THOR at this severity, it remains uncertain whether similar behaviour would have been observed. Next, the injury risk estimates were consistent across both THOR load cells, as the values were spatially positioned in similar regions relative to the IARBs (Fig. 6B-6C). Lastly, the model-estimated and measured load cell predictions of KTH injury risk using the IARB method showed strong agreement (Fig. G3).

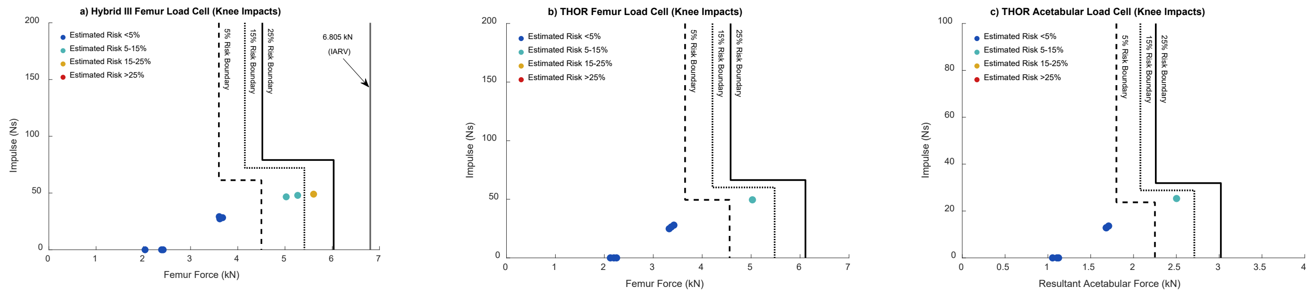

Fig. 6. Distribution of compressive femur force and impulse at each small female ATD load cell location measured during the experimental knee impact tests [36]. Injury risk distribution categorized by an estimated KTH injury risk <5%, 5-15%, 15-25%, and >25% per the IARB method.

To evaluate predictive performance, estimated KTH injury risks were compared to PMHS-derived risks across three impact velocities. As previously noted, the 2.5, 3.5, and 4.9 m/s PMHS tests resulted in no observed KTH injuries. Accordingly, estimated injury risk remained minimal: 0% at 2.5 m/s, 0.14±0.16% at 3.5 m/s, and 4.94± 4.22% at 4.9 m/s (Table 3). When evaluated against the PMHS baseline, all injury assessment methods estimated low KTH injury risks at 2.5 m/s. Specifically, the IARB methods derived in this study predicted risks averaging 0.00-0.01%, with the scaled HIII-5F IARB estimate for this impact velocity resulting in higher risks compared to the other IARBs (0.70%). Next, the experimental methods predicted 0% risk across all cases, whereas the conservative methods ranged from 0.01-0.03% with the Hybrid III femur load cell producing the highest estimates.

At 3.5 m/s, trends remained consistent. IARB methods estimated risks averaging 0.39-0.92%, experimental methods between 0.04-0.12%, and conservative approaches between 2.36-5.45%, with the highest values observed when applying the methods to the Hybrid III femur load cell.

At 4.9 m/s, where PMHS-derived injury risk increased to an average of 4.94 ± 4.22%, greater variation emerged. IARB methods predicted risks between 9.10-13.64%, with the scaled estimate slightly higher (15.94%). Experimental approaches estimated risks between 4.70-7.95%, aligning most closely with PMHS responses due to direct derivation from experimental KTH force transfer relationships. In contrast, conservative force-only methods produced the highest injury risks (38.99-50.16%), with the Hybrid III femur load cell exhibiting the greatest estimates.

TABLE III
COMPARISON OF ESTIMATED KTH INJURY RISK BY EACH APPROACH ACROSS EXPERIMENTAL DATA

Assessment Approach	*Subject*	*Load Cell Location*	*KTH Injury Risk for 2.5 m/s Tests (%)*	*KTH Injury Risk for 3.5 m/s Tests (%)*	*KTH Injury Risk for 4.9 m/s Tests (%)*
Cadaver-Based IRFs (Eq. 1-2)	*PMHS*	--	0.00 ± 0.00	0.14 ± 0.16	4.94 ± 4.22
IARB (Force + Impulse)	Hybrid III	Femur	0.01 ± 0.01	0.92 ± 0.09	13.64 ± 3.99
		Femur (Scaled) [8,31]	0.70 ± 0.23	3.98 ± 0.16	15.94 ± 3.08
	THOR	Femur	0.00 ± 0.00	0.39 ± 0.06	9.10
		Acetabulum	0.00 ± 0.00	0.47 ± 0.04	9.76
Experimental (Force Only)	Hybrid III	Femur	0.00 ± 0.00	0.12 ± 0.02	7.95 ± 3.46
	THOR	Femur	0.00 ± 0.00	0.04 ± 0.01	4.88
		Acetabulum	0.00 ± 0.00	0.04 ± 0.01	4.70
Conservative (Force Only)	Hybrid III	Femur	0.03 ± 0.02	5.45 ± 0.51	50.16 ± 9.26
	THOR	Femur	0.01 ± 0.00	2.36 ± 0.34	38.99
		Acetabulum	0.01 ± 0.00	2.80 ± 0.26	40.66

Comparison of KTH Injury Risk Assessment Methods using NCAP Data for Newer Model Year Vehicles

The NHTSA Vehicle Crash-Test Database was queried for full-frontal rigid-barrier tests at 56 km/h (35 mph) using the Hybrid III 5th-percentile adult female dummy in the right-front passenger seat. Eligible results were limited to US NCAP and NHTSA Research tests involving MYs 2010-2023, with valid femur-force data from both load cells. In these tests, the ATD was restrained by a three-point belt and positioned according to FMVSS No. 208 seating procedures [24,25]. The query yielded 565 vehicle tests, providing 1,130 femur-force measurements for analysis.

Fig. 9 illustrates the compressive femur force and impulse recorded across these load cell measurements, while Fig. 10 shows the impulse calculation methodology, following IIHS protocols for the midsize male [32]. Injury risk estimates were generally low (<25%), remaining well below the 6.805 kN IARV, except for the conservative force-only approach, which predicted some impacts exceeding the 25% KTH injury risk threshold (Table G7). This behaviour aligns with improvements in vehicle safety since the 1998-2004 MY vehicles used to derive the analytical simulation parameters [1,8], but is also likely influenced by the inclusion of belted tests, where forward knee excursions tend to be lower than in unbelted cases [31].

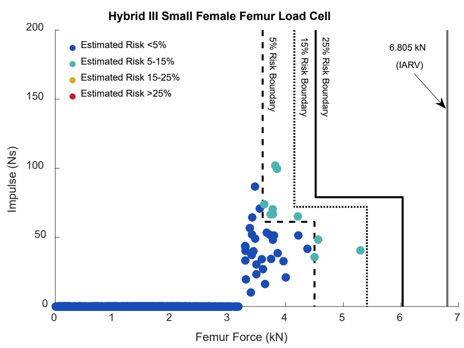

Fig. 7. Compressive femur force and impulse recorded using NCAP passenger data for the Hybrid III Small Female.

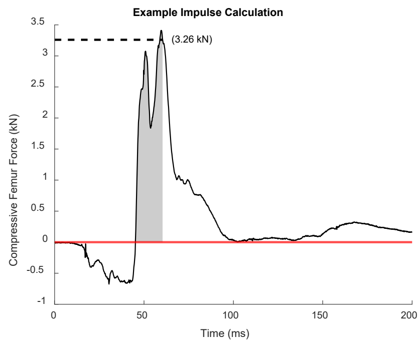

Fig. 8. NCAP impulse calculation logic for the Hybrid III Small Female femur load cell.

Since direct PMHS experimental data were unavailable for these tests, comparisons were made against overall injury trends in the field data, as done previously [8,31]. Hip injury risk was calculated for each load cell measurement as the minimum of the force- and impulse-based risks (Eq. 6). The combined KTH injury risk was then determined as the maximum of the hip and knee/distal femur risks per load cell measurement (Eq. 7). To account for asymmetrical loading, the final KTH injury risk was defined as the greater of the left- and right-side estimates.

Table 5 compares injury risk predictions across four assessment methods applied to NCAP passenger test data: the current IARB method, the scaled IARB approach, the experimental correction factor, and the conservative correction factor. Predicted KTH injury risks remained low across methods, with mean risk estimates below 1%, though ranges varied significantly. The conservative correction factor approach produced the widest range (up to 50.25%), while the experimental correction factor method predicted a maximum risk of 7.60%. The IARB and scaled IARB approaches estimated upper bounds of 13.41% and 15.79%, respectively.

TABLE V

ESTIMATED KTH INJURY RISK DISTRIBUTION FOR THE HIII-5F USING NCAP PASSENGER DATA (MODEL YEARS: 2010-2023)

Assessment Approach	*Hip Risk (Force) (%)*	*Hip Risk (Impulse) (%)*	*Knee/Distal Femur Risk (Force) (%)*	*Overall KTH Risk (%)*	*Risk Range (%)*
Current IARB	0.58 ± 3.14	0.43 ± 4.10	0.11 ± 0.72	0.20 ± 1.10	0.00 - 13.41
Scaled IARB [8,31]	0.38 ± 2.71	0.42 ± 4.54	0.68 ± 1.31	0.68 ± 1.31	0.00 - 15.79
Experimental (Force Only)	0.03 ± 0.35	--	0.01 ± 0.08	0.03 ± 0.35	0.00 - 7.60
Conservative (Force Only)	0.58 ± 3.14	--	0.11 ± 0.72	0.58 ± 3.14	0.00 - 50.25

Estimated injury modes varied across methods, as evident when comparing overall KTH risk to individual IRF averages. The scaled IARB approach primarily predicted knee/distal femur injuries, as impacts remained below the threshold where hip injury risk exceeded knee/distal femur risk, making overall KTH risk identical to knee/distal femur injury risk [8,31]. The experimental and conservative correction factor methods predominantly predicted hip injuries, as force-based hip injury risk exceeded knee/distal femur risk when applied to the same load cell, making overall KTH injury risk identical to hip injury risk. Lastly, the current IARB approach predicted a balanced distribution of knee/distal femur and hip injuries, with overall KTH risk falling between all three IRFs.

To compare injury risk estimates with real-world crash data, the dataset from [41] was analysed, with full search details provided in that publication. In summary, the NHTSA CISS database (collection years 2017–2022) was queried for single-event frontal crashes involving model year 2002 and newer vehicles where WinSmash-estimated ΔV was reported, focusing on belted drivers. The study excluded rollovers, fires, ejections, multi-impact events, unbelted occupants, and children under 13 years, resulting in 3,996 individual cases, representing approximately 3.9 million weighted cases. To align with the present analysis, the dataset was further refined to include only crashes involving MY 2010-2023 vehicles and female occupants, resulting in approximately 1.3 million weighted cases (Table 6).

TABLE VI

WEIGHTED KTH INJURY RISK (CALCULATED AS # OF INJURY CASES/# OF EXPOSURES) FOR AIS2+ INJURIES, (CISS 2017-2022, MY 2010-2023, FRONTAL, BELTED DRIVER, SINGLE EVENT)

Occupant	*Delta-V*	*Exposed*	*Injured*	*KTH AIS 2+ Risk*
All Females	*All Impacts*	1,361,003	1,777	0.13%
	High Severity Impacts (48-70 km/h)	22,569	427	1.89%
Small Females (143-162 cm)	*All Impacts*	280,412	326	0.12%
	High Severity Impacts (48-70 km/h)	2,798	159	5.69%

Weighted KTH AIS2+ injury risk remained low across all impact severities (0.13%), with an increase in high-severity crashes (1.89%). Comparing Tables 5 and 6, the IARB methods and conservative force-only approach overpredicted total KTH AIS2+ risk, though the current IARB method was closest. In high-severity crashes (ΔV 48-70 km/h), the methods underpredicted the weighted KTH injury risk based on average response, with the scaled IARB approach providing the closest estimate. The experimental force-only method underpredicted risk across all severities. Despite this, the injury risks determined via the field data were within the ranges predicted by each of the injury assessment methods. Lastly, refining the dataset to include only small females (defined as 143-162 cm [31]) did not significantly alter the comparisons. Injury risk across all impact severities was nearly identical (0.12%), and the risk in high-severity crashes was similarly elevated (5.69%). However, injury risk was notably higher for smaller females compared with the broader female population.

IV. DISCUSSION

Using a combination of experimental testing and analytical simulation data for both female cadavers and ATDs, different injury assessment methods were explored to identify a suitable approach, as current approaches rely on scaling the midsize male results or are absent altogether [8,10]. To do so, three approaches that are currently utilized for the midsize male ATDs were explored, each derived from experimental or analytical force transfer relationships between subjects.

Discussion on the Experimentally Derived KTH Injury Assessment Method

The first method used experimentally derived correction factors from force transfer relationships reported in [36], applied directly to knee/distal femur and hip IRFs. This approach reflects traditional methodologies and serves as the foundation for current IRFs and IARVs in US NCAP and FMVSS No. 208 tests [10,11,23]. It is based on two key assumptions. First, knee/femur injuries are assumed to be more likely than hip injuries for a given force, a conclusion drawn from tolerance tests that demonstrated a high prevalence of knee/femur injuries and relatively few hip injuries [11,22]. Second, the cadaver-based KTH IRF is assumed to be directly applicable to the Hybrid III femur load cell ($T_{knee} = 1.000$), which comes from observations that the femur load cell force was roughly equivalent to the PMHS applied force under similar experimental conditions [10,23].

Applying these assumptions to the Hybrid III small female ATD results in a comparable interpretation of KTH injury risk relative to the original KTH IRFs and IARVs. Experimentally, the applied PMHS knee force was slightly lower than the Hybrid III femur load cell force ($T_{knee} = 0.92$) but remained reasonably close to a ratio of 1 in the tests reported by [36]. This supports the assumption that the Hybrid III femur load cell represents the PMHS applied knee force, which allowed the original KTH IRFs to be applied outright [10,11,22,23]. However, evolving research has expanded our understanding of KTH injuries, influencing the applicability of these initial IRFs.

When tested in isolation, the hip has the lowest force tolerance along the KTH region [14,15]. In KTH IRFs derived from tolerance tests, a given level of hip injury risk generally corresponds to a lower risk of knee/distal femur injury. This principle forms the basis for determining lower and upper force limits in the KTH IARBs, reinforcing the need to consider both knee/femur and hip IRFs in injury risk assessments. Notably, reliance solely on the knee/distal femur IRF may underestimate overall KTH injury risk in specific scenarios. This limitation was consistently observed in Hybrid III simulations, where femur load cell outputs were used for both KTH IRFs. As a result, peak force values could not generate higher knee/distal femur injury risk predictions, given that the hip IRF consistently indicated greater injury risk for the same femur load cell force (Fig. D1-D2). For the THOR ATD, which measures forces in both the femur and acetabulum, predicting a higher knee/distal femur injury risk is theoretically possible with the given IRFs. However, this would require significant variation in the femur-to-hip force transfer ratio ($r_{TH_{THOR}}$), which was not observed in the present study.

This distinction is critical because current KTH assessments in FMVSS No. 208 and the US Frontal NCAP only evaluate femur fracture risk based on peak compressive force, using an IRF more suited for evaluating knee/distal femur injury risk [8,11]. Consequently, continued use of these values likely underestimates overall KTH injury risk, particularly for hip injuries, which carry a greater societal burden than knee/distal femur injuries [1,2,8,13]. Furthermore, the present analysis suggests that current IARVs, which correspond to roughly a 35% risk of knee/distal femur injury [11], are becoming increasingly insensitive within the modern vehicle landscape. While this reduced sensitivity can partly be attributed to advancements in automotive safety, excluding hip force tolerance and loading duration dependence from IARVs may introduce unintended consequences.

Newer countermeasure designs aimed at minimizing knee force and maximizing energy absorption could inadvertently reduce ATD load cell forces below prescribed limits while extending loading duration enough to elevate hip injury risk. This effect would not be captured by force-based limits alone, particularly when using an IRF that does not account for hip injury risk. Additionally, analytical simulations were conducted using unrestrained subjects. As shown in this study and a similar analysis performed by [31], KTH injury risks derived from belted test conditions tend to underestimate the actual injury risk observed in real-world crashes involving belted occupants at similar severities. This discrepancy likely stems from reduced knee-to-knee bolster interaction caused by belt restraints limiting the subject's forward excursion compared to unbelted cases [31].

As a result, the underprediction bias identified in the experimental correction factor approach across analytical simulations using unrestrained conditions, led to even greater KTH injury risk underestimation for belted occupants in NHTSA vehicle tests. Furthermore, it was the only method to underpredict total AIS 2+ KTH injury risk in those tests, regardless of impact severity, making it less ideal for injury assessment. To address these concerns, continued adoption of assessment methodologies that integrate both force magnitude and loading duration, consistent with recommendations from [8] and seen in current IIHS [32] and EuroNCAP [42] protocols, would help mitigate the risk of shifting injury trends toward the hip or further underestimating belted-KTH injury risk. These protocols also establish KTH injury risk thresholds as low as 5%, enhancing sensitivity in KTH injury assessments [32,42].

Discussion on the KTH Injury Assessment Reference Boundary Method

The second approach represents the most updated understanding of KTH injuries. Using the results of analytical simulations that spanned more severe NCAP and FMVSS 208 tests on 1998-2004 MY vehicles, a set of IARBs were derived for each ATD load cell. This approach was established for the Hybrid III midsize male by [8], using a conservative correction factor to define the smallest load cell force histories associated with a given risk of KTH injury in the female cadavers over the range of simulated parameters. To account for differences in force tolerance between the knee/distal femur and hip, the boundaries were split into upper and lower force limits. Recognizing that hip injuries typically arise from lower-rate, longer-duration loading, impulse was incorporated into the assessment to bridge these limits and establish realistic bounds, thereby reducing the overprediction of KTH injury inherent in the conservative force-only approach.

Comparison of the final Hybrid III small female IARBs with the scaled response presented in [8] indicates a broadly similar assessment of KTH injury risk despite using different data sets, providing further confidence in the updated small female IARBs (Fig. 5, Table E1). Differences between boundaries arise from slight variations in the derivation of the force limits. Mainly, it was not feasible for [8] to adapt the original knee/distal femur IRF for use with the small female, necessitating scaling of the male values. This led to upper force limits falling below the corresponding lower force limits at the 3% risk level, contradicting the intended interpretation of these thresholds. Additionally, transition impulses could not be defined for the 3% and 5% risk levels because the upper and lower force limits were too close to establish a meaningful distinction [8].

Scaling had the greatest impact in the NCAP analysis, where nearly all impacts were relatively low-risk exposures, causing the scaled approach to primarily predict knee/distal femur fractures due to greater sensitivity in that IRF range. This also explains why the scaled IARB yielded the highest injury risk estimates, surpassing even the conservative approach, since the heightened sensitivity of the scaled knee/distal femur IRF dictated lower-risk response predictions (Fig. E4). In contrast, the updated IARB applied to the same dataset distributed injury risk across both knee/distal femur and hip injuries, better reflecting real-world crash proportions [2,31,33]. Analysis of the analytical simulations and experimental knee impact tests further validated this conclusion, with the current IARBs demonstrating closer alignment with PMHS injury risk estimates compared to the scaled IARB. This suggests that the Knee/Femur IRF presented in this work may be more suitable for use with female subjects compared to scaling approaches, although this should be continuously re-evaluated as more female-specific injury data becomes available.

Incorporating impulse alongside peak load cell force provides a more practical representation of KTH injuries by accounting for both loading magnitude and duration. This suggests that the IARB methodology offers a more balanced approach to sensitivity and specificity, which is particularly important for ATDs that cannot inherently distinguish between these factors. However, limitations remain. Since the IARB approach was developed using one-dimensional analytical models, its applicability is influenced by model assumptions and the specific simulation parameters used. Each boundary optimizes the combination of force and impulse measurements for a specified KTH injury risk but does not guarantee complete predictive accuracy across all ATD peak force and impulse conditions.

The primary source of uncertainty arises when peak load cell forces fall between the upper and lower force limits, in which case risk prediction depends on the validity of the transition impulse derivation [8]. This derivation, which is not part of the original force-based IRFs, uses the Hip IRF and analytical modelling to account for biofidelity differences resulting from variations in knee bolster penetration and KTH force transfer between ATDs and PMHS (i.e., recognizing that multiple ATD load cell force histories can correspond to a single PMHS KTH force history) [8]. While this approach serves to enhance specificity compared to just using the conservative (force-only) approach, it also means that improvements in ATD biofidelity, or deviations from the original simulation assumptions or transition impulse definitions, could directly affect the validity of the IARBs. This is discussed further in the following sections.

Despite these limitations, the benefits of the combined force and impulse approach are evident in the results shown across the various data sources analysed in the present work. The IARB method consistently predicted the least variation in injury risk distribution across subjects and measurement locations. In the analytical simulation dataset, the IARB method outperformed force-only approaches, achieving higher R^2 values (ranging from 0.69 to 0.77), lower RMSEs, and smaller positive biases (9.8-12.4), demonstrating strong correlation with PMHS-based injury estimates. In contrast, the conservative correction factor approach exhibited poor predictive performance, with negative or low R^2 values (as low as -0.21 for the Hybrid III femur), higher RMSEs, and substantial positive biases, indicating a strong tendency to overpredict KTH injury risk. This overprediction can also problematic, as it does not necessarily reflect real-world injury risk and may lead to hyper-optimization of safety systems, inadvertently shifting exposure to more fatal injury regions, such as the head or chest. Similarly, in the knee impact tests, the current IARB approach produced estimates most closely aligned with PMHS KTH injury risk, aside from the experimental approach, which was derived directly from the dataset and therefore expected to be the closest in value. Evaluating the NCAP data further supported this conclusion, showing that the Hybrid III IARB predicted low overall risk estimates (0.20±1.10%), that most closely matched the overall weighted AIS 2+ KTH injury risk (0.13% and 0.12% for females and small females, respectively), but below the weighted risk at higher impact severities (1.89% and 5.69% for females and small females, respectively), although this trend was also present in the previous analysis by [31], and was consistent across all assessment methodologies.

Discussion on Using the Conservative Impact Assumption Without Incorporating Impulse

The last approach follows efforts by [1] to establish KTH criteria for THOR-50M, adapting the conservative correction factor approach of [8], but omitting impulse due to the lack of knee impact data comparable in severity to FMVSS No. 208 and US NCAP crash tests, which informed the Hybrid III values. Recent literature has suggested that the THOR-50M adaptation largely overestimates KTH risk [12] and thus may not be practical for KTH injury assessment, prompting further investigation.

The work by [1] yielded correction factors of 1.3 for T_{knee} (femur load cell) and 1.429 for T_{Hip} (acetabular load cell). For the THOR-05F in this study, similar calculations yielded 1.23 for T_{knee} and 1.40 for T_{Hip}, showing minimal differences between estimates, and nearly identical force transmission to the THOR-50M values reported in [39]. These similarities suggest that the contrast between the observations of [12] and the IARB method of [8] stem from the decision to not incorporate impulse. Without impulse, the approach becomes far more prone to unrealistic injury estimates due to extreme sensitivity without specificity (i.e. it will tend to produce higher injury risk estimates, with little confidence as to whether the estimate represents a true positive or false positive). This was apparent in the present work where the conservative approach alone estimated a high risk of KTH injury when applied to ATD impact tests from [36], despite PMHS data indicating minimal risk (<5%) and no observed KTH injuries [37]. The analytical simulation analysis further highlighted this issue, with the conservative approach showing substantial overprediction biases, high RMSE values, and low R^2 values when compared to PMHS risks. In contrast, other methodologies produced injury risk estimates that better correlated with the PMHS values across both datasets, reinforcing the shortcomings of the force-only approach when impulse is omitted.

To address these limitations in the current THOR-50M KTH injury assessment methodology, the THOR-05F IARBs developed in this study were scaled to estimate preliminary IARBs for the THOR-50M (Table E3). Given the similarities between the transition impulses for the Hybrid III small female and the scaled values presented in [8], and between the KTH force transmission in the THOR-05F and THOR-50M [39], scaling from the THOR-05F likely provides reasonable approximations. However, it is important to note that the original IARB method relied on scaling factors specific to the Hybrid III [8]. For the THOR-05F, NHTSA departed from this precedent, citing concerns about the unclear basis for the original Hybrid III KTH scale factor [40]. Consequently, the THOR-05F KTH complex was designed using different scaling assumptions, resulting in an impulse scaling factor of 0.68 (or 1.47 when expressed inversely). Without THOR-50M-specific impact data and modelling, transition impulses for THOR-50M could align more closely with Hybrid III value [8], though design differences and updated scaling techniques suggest otherwise. Future research should focus on validating and refining these preliminary THOR-50M IARBs.

Beyond the IARB methodology, results suggest that using experimentally derived correction factors or cadaver-derived IRFs directly would improve injury risk estimates for THOR-50M in unrestrained cases. Experimentally derived correction factors for the THOR-05F averaged 0.97 for T_{knee} using the femur load cell, and 1.06 for T_{Hip} using the acetabular load cell, both close to a value of 1, indicating minimal adjustment needed for these impact conditions. This aligns with [12], which found that lowering the correction factor from 1.429 to 1 improved consistency in injury risk between ATD and PMHS simulations. With that said, incorporating impulse remains a more robust representation of KTH injuries compared to methods using the peak load cell force alone [8].

Considerations with the KTH IRFs Reported in This Work

The goal of this study was to develop female-specific KTH injury assessment methods, as recent studies show that females have higher odds of KTH injuries [33,34]. The findings were informed by non-injurious experimental knee impact tests and one-dimensional analytical models, adapting work done previously for midsize males [7,8].

The current efforts provide the most representative information for assessing KTH injuries in small female ATDs, filling a significant knowledge gap. Further, the similarity in the injury assessment approaches across test series suggests that the current small female adaptations are reasonable given the assumptions used to define each approach. However, the results are bound by the assumptions and data used, and the small female adaptations, although reasonable, do not ultimately support the persistence of the KTH injury disparity across sex. Therefore, it is important to continually reevaluate the current findings.

Importantly, the injury data informing the KTH IRFs were primarily from tests on male subjects [1,14,15]. This means the current IRFs classify a “small female” based on provided covariates, but they may not fully reflect the KTH injury risk for small female cadavers. This presents a limitation in accurately predicting female-specific injury risks, particularly for the lower extremities, where sex-based differences in geometry, bone density, and soft tissue compliance have been documented [43].

This limitation highlights the broader underrepresentation of females in biomechanical testing, which continues to complicate efforts to understand and address sex-based disparities in injury outcomes. Future research should focus on improving the robustness and accuracy of KTH injury risk functions by incorporating more female-specific injury data. This includes developing updated tolerance curves through dedicated testing of small female subjects and continually refining both physical and computational assessment tools to more accurately represent female anatomy and biomechanical response. These efforts are essential for strengthening confidence in current assessment methods and for ensuring that the injury criteria used in crash safety evaluations are appropriate for the intended populations. If future investigations reveal deviations from the results presented here, the injury assessments can and should be revised accordingly and can follow the methodology outlined in this study.

Considerations of the Current Methods when Applied to Tests with Belted ATDs

In this study, injury risk assessment methods were compared to real-world crash data from the NHTSA CISS database using the dataset from [33]. The analysis showed that overall, belted injury risk for female drivers in 2010-2023 MY vehicles was low when examining all impact severities (0.13%), with a slight increase when limiting the data to higher severity impacts with a delta-v of 48-70 km/h (1.89%). Further refining the dataset to examine small females revealed nearly identical injury risks when looking at the aggregated risk across all impact severities (0.12%). However, in higher-severity crashes, the injury risk increased to 5.69%, which was higher when compared against the broader female population. These results align with ATD predictions in Table 5, with injury assessment methods more accurately estimating overall KTH injury risk across all impact severities than risks observed in high-severity crashes similar to NHTSA NCAP and research tests at 56 km/h.

Compared to a previous NASS-CDS analysis (1993–2007) by [31], the present study shows lower KTH injury risks. Prior estimates indicated injury rates of ~3% for belted small females, rising to ~20% in high-severity frontal impacts. Similarly, frontal impact tests with the Hybrid III small female ATD yielded a 3.14% risk, with only one test exceeding 25% risk when applying the scaled IARB method. These findings align with recent literature showing declining KTH AIS 2+ injury risk in newer vehicles [33,34]. However, the decline was not proportional, as risk reductions were more pronounced across all severities (3% vs. 0.12%) than in high-severity impacts (20% vs. 5.69%), potentially due to smaller sample sizes when limiting accidents to small females in newer vehicles.

Beyond sampling limitations, the consistency across studies and the disparity in injury risks at different severities raise key questions about the impact of seatbelt usage on current KTH assessment methods. Analytical simulations and knee impact tests largely controlled the initial impact conditions, allowing injury assessment methods to estimate risk under relatively matched conditions. However, the consistent underprediction bias in belted tests suggests that certain belt interactions or real-world crash factors are not fully captured with the current methods. For example, even the conservative force-only approach, which substantially overpredicted KTH risk in unbelted cases, underestimated high-severity KTH injury risk in belted scenarios.

Recent research suggests that BMI may contribute to sex-specific disparities in lower extremity injury risk by influencing seatbelt interaction [44,45]. Jones et al. [44] found that sex-related differences in body shape led to increased belt webbing usage in females, resulting in suboptimal lap belt engagement with the ASIS. This improper belt engagement could lead to greater forward knee excursions and an increased risk of submarining. Brumbelow [45] observed minimal sex differences in lower extremity injury risk at low BMI but identified significant disparities at higher BMI, with injury risk increasing further as ΔV increased. In a subject-specific study of female KTH force transfer by [37], BMI did not influence force transfer amongst the subjects. However, these tests were conducted in a free-back condition without a seatbelt, reinforcing the idea that BMI's influence on injury risk may be specific to belt engagement.

If female occupants experience poor belt interaction and increased knee excursions not captured by ATDs, load cell forces used to estimate KTH injury risk may not accurately reflect human loading conditions. Additionally, unaccounted submarining compromises hip posture assumptions in the Hip IRF, as changes in hip angle significantly alter joint coverage and local stress distributions during impact. Studies show deviations from neutral hip posture can reduce hip fracture tolerance by as much as 30-40% [14,27,43]. Thus, while overall KTH injury rates are declining, future research should assess whether current methods adequately capture small female injury risk in belted scenarios, as sex-specific considerations may necessitate refinements. Potential modifications include refining pre-impact positioning assumptions used for the Hip IRF, introducing correction factors for ATD pelvis orientation, or conducting additional tests to evaluate knee bolster penetration differences in belted versus unbelted conditions. Enhancing the biofidelity of small female ATDs would also help address these discrepancies and will be further discussed in the next section regarding the THOR ATD.

Considerations with Future Improvements to THOR Biofidelity

The findings presented in this study, particularly those related to the THOR ATDs, reflect the current state of these devices. NHTSA continues to pursue advancements in the biofidelity, durability, and usability of the THOR suite of ATDs to enhance injury assessment in modern vehicle crashes and improve sensitivity to evolving restraint systems. For KTH loading, this requires modifying ATDs to better replicate forward knee excursions, bolster penetration, and applied knee force under comparable conditions. These refinements could also enhance THOR's ability to assess submarining risk but remain challenging. As shown in Fig. 1 and Table C6, the THOR ATD's stiffer construction leads to greater bolster penetration and higher initial knee forces than the PMHS, except when force-limiting bolsters are used. To address this external biofidelity discrepancy, the internal KTH complex was previously tuned using midsize male data to better align acetabular load cell forces with PMHS results. This adjustment represents a trade-off, modifying internal biofidelity to compensate for external response differences.

As emphasized throughout this paper, correction factors lose effectiveness when applied beyond the specific conditions under which they were derived. While external force response variations may not significantly affect individual internal KTH force transmission, such as the THOR knee-to-hip force transmission remaining around 40% regardless of knee bolster condition, they indirectly affect the consistency of these relationships across subjects. Tuning internal biofidelity without improving external biofidelity thus limits the singular correction factor approach. The IARB method currently remains the most robust solution, as it introduces mechanical nuance to address current ATD-specific biofidelity limitations.

Future improvements should focus on enhancing ATD external biofidelity, particularly bolster deformation and knee force response, while simultaneously refining the internal biofidelity of the KTH complex to allow direct application of cadaver-derived IRFs to ATD load cell outputs. Without internal calibration, even with perfectly matched external impact conditions (equal peak forces across conditions), the THOR acetabular load cell would likely continue to underpredict peak PMHS hip force. Current results indicate that approximately 40% of knee force is transmitted to the THOR acetabular load cell, compared to ~56% in PMHS (Table 1).

If only the external response is improved, the conservative correction factor approach presented in this analysis (which assumes equivalent knee forces across subjects) may be a more practical solution, provided that internal KTH force transmission remains largely unaffected by the external modifications. Ultimately, continued refinement of the THOR design will require periodic reassessment of injury assessment strategies and may necessitate revisions to current IARBs or enable other simplified correction factor approaches, such as direct application of cadaver-based IRFs.

Influence of Inter-Subject Variation on the Assessment Methods Derived in this Work

The correction factors and IARBs developed to relate small female ATD load cell measurements to PMHS response are based on averaged anthropometric properties from autopsy data, raising concerns about their applicability to a broader population. While individual differences exist amongst subjects, their combined impact on knee-to-hip force transfer percentage was minimal at the population level during the unrestrained loading conditions analysed in the present body of work. Across experimental test data and analytical simulations, the force transferred from the knee to the hip remained around 55-56%, largely unaffected by individual subject variation. Similar trends were also observed during midsize male testing, where the experimental data predicted a knee-to-hip force transfer of 54% and the simulations predicted a force transfer of 55% [7], closely aligning with the female percentages despite differences in subject sex, mass, and stature.

This consistency reinforces confidence that the final injury assessment methodologies are reasonable adaptations of midsize male approaches, which are widely used in the literature. Additionally, it suggests that estimating THOR-50M IARBs from THOR-05F data is a valid approximation, assuming the scaling techniques used for THOR-05F to THOR-50M remain accurate and no major modifications are made to the ATDs. Importantly, however, this claim is largely limited to unbelted conditions, as both the current findings and recent literature regarding the sex-based KTH injury disparity indicate that intersubject variability in mass and mass coupling may have a greater influence on KTH force transfer and injury patterns in belted conditions [45]. Thus, while future refinements should focus on exploring the effect of intersubject variability on KTH force transfer with belted occupants, the correction factors and IARBs developed here provide a reasonable and representative foundation for small female injury assessment previously only obtainable through scaling methods.

Additional Considerations for the Assessment Methods Derived in this Work

It is important to emphasize that the KTH impact behaviour for all subjects analysed throughout this test series was investigated using a simplified experimental setup involving symmetric knee loading in an upright, free-back posture. This configuration mirrors previous KTH studies on midsize male PMHS and ATDs [7,8], enabling a systems-level analysis of KTH force transmission by isolating fundamental inertial responses while minimizing variability introduced by subject positioning, restraint interaction, and complex vehicle environments. This simplified condition provides a well-controlled framework to independently develop small female injury assessment methodologies using established techniques, rather than relying on scaled male data. It also enables direct comparison of force transfer behaviour between male and female subjects to identify sex-specific differences in the inertial response.

However, while this approach allows for consistency across test series, it does not account for several relevant factors that can influence injury outcomes in real-world crashes. For example, muscle activation has been shown to increase the likelihood of femoral shaft fractures by 20-40% [26,46], due to increased compressive preload and altered dynamic stiffness in the thigh. Variations in mass distribution and soft tissue compliance across individuals and between sexes can also influence both energy absorption and the timing of load transfer, potentially delaying or attenuating the force transmitted to the hip [7,36]. Asymmetric knee impacts further complicate the loading scenario. These conditions change the initial mass coupling, increasing the effective mass behind the hip on the side with greater force application. This not only raises the magnitude of force transmitted to the hip but may also introduce torsional components in the load path [7,8], which are not accounted for under symmetric assumptions.

Although these factors fall outside the scope of this study, they must be considered when interpreting findings in real-world contexts. Regulatory testing protocols, which primarily assess symmetric loading in standard automotive postures, are less affected by these limitations [1,8,32]. However, future automotive trends, such as highly autonomous vehicles (HAVs), could alter the applicability of these results. Occupants in HAVs will assume passenger roles, likely deviating from standard automotive postures around which current restraint systems are designed [47]. In the context of this study, a more reclined posture would primarily affect hip positioning at the time of impact, thereby influencing the hip IRF used in Eq. 2, which currently assumes a hip flexion angle of 15°, as established in [1]. Additionally, deviations in occupant posture may alter knee excursion paths, increasing the risk of suboptimal or premature interaction with restraint systems. For example, premature contact with a knee airbag, triggered by an unexpected occupant trajectory, could result in elevated loading rates at the knee/distal femur. This premature engagement may cause immediate failure due to localized force concentration, occurring before the knee-bolster restraint system can effectively mitigate the impact energy.

Future research should continue assessing the applicability of KTH injury criteria across varied postures and loading conditions, particularly if regulatory seating positions evolve in response to HAV adoption. This evolution in occupant behaviour and vehicle design extends beyond physical testing and increasingly incorporates virtual assessments using human body models (HBMs). These models offer improved anatomical accuracy and help address some limitations of physical surrogates, such as excessive bolster penetration caused by the stiffness of ATDs. They also provide the flexibility to simulate a wide range of occupant conditions, including variations in posture, impact orientation, and physiological characteristics, many of which would be impractical or costly to evaluate through physical testing alone.

Despite their advantages, the authors do not anticipate that HBMs will fully replace physical testing. Physical ATDs remain essential due to their simplicity, repeatability, and the extensive historical data available for benchmarking automotive safety performance. Therefore, it is critical to explore KTH force transfer behaviour between PMHS and HBMs using methodologies similar to those applied in the present study. These comparisons can then be extended to assess the effects of occupant variability in posture and anthropometry. Thus, looking ahead, a combined approach that leverages physical ATDs for standardized crash assessments while employing HBMs to demonstrate robustness of safety systems across more conditions than feasibly testable with physical surrogates will likely provide the most comprehensive framework for occupant safety evaluation.

V. CONCLUSIONS

This study investigated methods for relating ATD load cell forces to KTH injury risk in female occupants using experimental data and analytical modelling. Three approaches, adapted from those previously developed for midsize male ATDs, were applied to small female ATDs. The correction factors and reference values aligned with prior research, including scaled estimates derived from the HIII-50M. Injury assessments were conducted using analytical simulations, experimental testing, and US NCAP passenger data.

Overall, the results support the adoption of assessment methodologies that incorporate both force magnitude and loading duration for small female KTH injury evaluation, consistent with current IIHS and Euro NCAP protocols. Given the external and internal biofidelity differences across subjects, incorporating impulse is essential to balance the sensitivity and specificity of the ATDs in their current state, particularly as vehicle restraint systems evolve to mitigate lower extremity injuries. While further refinement will be necessary as additional female-specific biomechanical data become available and updates are made to the THOR-05F design, the methodology presented here provides a validated and enhanced framework for assessing small female KTH injury risk. This work addresses a critical knowledge gap by developing injury assessment methods tailored for small female ATDs, improving the accuracy and applicability of KTH injury evaluation for diverse occupant populations.

In addition, preliminary IARB thresholds for the THOR-50M were proposed in the absence of established values, and future work should explore the behaviour and robustness of these IARBs across various datasets, similar to the approach used in this study. Finally, the framework established here provides a foundation for future research, particularly if HAVs alter standard automotive seating configurations.

VI. ACKNOWLEDGEMENT

The following research was funded by the National Highway Traffic Safety Administration (NHTSA) under contract number DTNH2215D00022. The authors would also like to thank the staff at the University of Virginia's Center for Applied Biomechanics for all their help in this test series.

VII. REFERENCES

[1] Craig, M., Parent, D., et al. Injury Criteria for the THOR 50th Male ATD, N.H.T.S. Administration, Editor. 2020: Washington, DC, USA.

[2] Kuppa, S. and Fessahaie, O. An overview of knee-thigh-hip injuries in frontal crashes in the United States. *Proceedings of Proceedings of the 18th International Technical Conference on Experimental Safety Vehicles*, 2003. National Highway Traffic Safety Association, Washington DC

[3] Rudd, R., Scarboro, M., and Saunders, J. Injury Analysis of Real-World Small Overlap and Oblique Frontal Crashes. *Proceedings of Proceedings of the 22nd International Technical Conference on the Enhanced Safety of Vehicles*, 2011.

[4] Rupp, J.D. Biomechanics of Hip Injuries in Frontal Motor-Vehicle Crashes. 2006, University of Michigan.

[5] Rupp, J.D., Reed, M.P., et al. The tolerance of the human hip to dynamic knee loading. *Stapp Car Crash J*, 2002. 46: p. 211-28

[6] Rupp, J.D., Miller, C.S., et al. Characterization of Knee Impacts in Frontal Crashes, in *20th International Technical Conference on the Enhanced Safety of Vehicles (ESV)*. 2007: Lyon, France.

[7] Rupp, J.D., Miller, C.S., et al. Characterization of knee-thigh-hip response in frontal impacts using biomechanical testing and computational simulations. *Stapp Car Crash J*, 2008. 52: p. 421-74

[8] Rupp, J.D., Reed, M.P., Miller, C.S., Madura, N.H., and Klinich, K.D. Development of New Criteria for Assessing the Risk of KTH Injury in Frontal Impacts Using Hybrid III Femur Force Measurements, in *Proceedings of the 21st (ESV) International Technical Conference on the Enhanced Safety of Vehicles*. 2009, National Highway Traffic Safety Administration: Stuttgart, Germany.

[9] Newton, I., "Philosophiae naturalis principia mathematica". 1687: Londini: Jussu Societatis Regiæ.

[10] Eppinger, R.H., Sun, E., et al. Development of improved injury criteria for the assessment of advanced automotive restraint systems—II, N.H.T.S. Administration, Editor. 1999: Washington, DC.

[11] Kuppa, S., Wang, J., Haffner, M., and Eppinger, R. Lower Extremity Injuries and Associated Injury Criteria, in *International Technical Conference on Enhanced Safety of Vehicles*. 2001.
[12] Peres, J. and Praxl, N. A Simulation Study on the Knee-Thigh-Hip Loading of the THOR Compared to Human Body Models. *Proceedings of Enhanced Safety of Vehicles Conference*, 2023. Yokohama, Japan
[13] Yoganandan, N., Nahum, A.M., and Melvin, J.W., "Accidental Injury: Biomechanics and Prevention". Third ed. 2015: Springer.
[14] Rupp, J.D., Flannagan, C.A., and Kuppa, S.M. An injury risk curve for the hip for use in frontal impact crash testing. *J Biomech*, 2010. 43(3): p. 527-31
[15] Rupp, J.D., Flannagan, C.A., and Kuppa, S.M. Injury risk curves for the skeletal knee-thigh-hip complex for knee-impact loading. *Accid Anal Prev*, 2010. 42(1): p. 153-8
[16] Patrick, L.M., Kroell, C.K., and Mertz, H.M. Forces on the Human Body in Simulated Crashes, in *Proceedings of the Ninth Stapp Car Crash*
Conference. 1965: Minneapolis, MN. p. 237–259.
[17] Melvin, J. and Nusholtz, G. Tolerance and response of the knee-femur-pelvis complex to axial impacts—impact sled tests. 1980, The University of Michigan: Highway Safety Research Institute.
[18] Melvin, J. and Stalnaker, R. Tolerance and response of the knee-femur-pelvis complex to axial impact. 1976, University of Michigan: Highway Safety Research Institute.
[19] Melvin, J.W., Stalnaker, R.L., Alem, N.M., Benson, J.B., and Mohan, D. Impact Response and Tolerance of the Lower Extremities, in *Proceedings of the Nineteenth Stapp Car Crash Conference*. 1975, Society of Automotive Engineers.
[20] Powell, W.R., Advani, S.H., Clark, R.N., Ojala, S.J., and Holt, D.J. Investigation of Femur Response to Longitudinal Impact. *Proceedings of Proceedings of the Eighteenth Stapp Car Crash Conference*, 1974.
[21] Powell, W.R., Ojala, S.J., Advani, S.H., and Martin, R.B. Cadaver Femur Responses to Longitudinal Impacts. 1975, SAE International.
[22] Morgan, R., Eppinger, R., and Marcus, J. Human Cadaver Patella-Femur-Pelvis Injury due to Dynamic Frontal Impact to the Patella. 1989.
[23] Morgan, R.M., Eppinger, R.H., Marcus, J.H., and Nichols, H. Human Cadaver and Hybrid III Responses to Axial Impacts of the Femur. *Proceedings of International Research Council on the Biomechanics of Injury*, 1990. Bron, France
[24] Regulations, U.S.C.o.F. Title 49, Part 571.208: Federal Motor Vehicle Safety Standards; Occupant Crash Protection, D.o. Transportation, Editor. 2025, National Highway Traffic Safety Administration: Washington, D.C.
[25] Regulations, U.S.C.o.F. Title 49, Part 572, Subpart O: Anthropomorphic Test Devices; Hybrid III 5th Percentile Adult Female Dummy, D.o. Transportation, Editor. 2025, National Highway Traffic Safety Administration: Washington, D.C.
[26] Chang, C.Y., Rupp, J.D., Kikuchi, N., and Schneider, L.W. Development of a finite element model to study the effects of muscle forces on knee-thigh-hip injuries in frontal crashes. *Stapp Car Crash J*, 2008. 52: p. 475-504
[27] Rupp, J.D., Reed, M.P., Jeffreys, T.A., and Schneider, L.W. Effects of hip posture on the frontal impact tolerance of the human hip joint. *Stapp Car Crash J*, 2003. 47: p. 21-33
[28] Rupp, J. Biomechanics of Hip Injuries in Frontal Motor-Vehicle Crashes. 2006.
[29] Rupp, J.D., Flannagan, C.A., and Kuppa, S.M. Development of new injury risk curves for the knee/distal femur and the hip for use in frontal impact testing. 2009: University of Michigan Transportation Research Institute.
[30] Rupp, J.D., Miller, C.S., et al. Characterization of Knee Impacts in Frontal Crashes. *Proceedings* 2007.
[31] Kirk, K. and Kuppa, S. Application and Evaluation of a Novel KTH Injury Criterion for the Hybrid III Dummy in Frontal Crash Test Environments, in *21st International Technical Conference on the Enhanced Safety of Vehicles*. 2009, National Highway Traffic Safety Administration: Washington, DC.
[32] Safety, I.I.f.H. Moderate Overlap Crashworthiness Evaluation 2.0 Rating Guidelines: Version II. 2024.
[33] Forman, J., Poplin, G.S., et al. Automobile injury trends in the contemporary fleet: Belted occupants in frontal collisions. *Traffic Inj Prev*, 2019. 20(6): p. 607-612
[34] Brumbelow, M.L. and Jermakian, J.S. Injury risks and crashworthiness benefits for females and males: Which differences are physiological? *Traffic Inj Prev*, 2022. 23(1): p. 11-16
[35] Nutbeam, T., Weekes, L., et al. Sex-disaggregated analysis of the injury patterns, outcome data and trapped status of major trauma patients injured in motor vehicle collisions: a prespecified analysis of the UK trauma registry (TARN). *BMJ Open*, 2022. 12(5): p. e061076
[36] Carpenter, R.L., Berthelson, P.R., Donlon, J.P., and Forman, J.L. Comparison of the Knee-Thigh-Hip Response in Small Female ATDs with Female PMHS, in *Proceedings of the International Research Council on the Biomechanics of Impact (IRCOBI)*. 2024: Stockholm, Sweden. p. 243-273.
[37] Carpenter, R.L., Berthelson, P.R., Donlon, J.P., and Forman, J.L. Quantifying Female Subject-specific Knee-thigh-hip Responses in Frontal Impact Scenarios, in *Proceedings of the International Research Council on the Biomechanics of Impact (IRCOBI)*. 2023: Cambridge, United Kingdom. p. 978-1012.
[38] Fryar, C.D., Carroll, M.D., Gu, Q., Afful, J., and Ogden, C.L. Anthropometric Reference Data for Children and Adults: United States, 2015-2018. *Vital Health Stat 3*, 2021. 3(36): p. 1-44
[39] Martin, P.G. and Scarboro, M. THOR-NT: Hip Injury Potential in Narrow Offset and Oblique Frontal Crashes, in *22nd International Technical Conference on the Enhanced Safety of Vehicles (ESV)*. 2011: Washington D.C. p. 16.

[40] Lee, E.L., Parent, D.P., Craig, M.J., McFadden, J., and Moorhouse, K. Biomechanical Response Requirements Manual: THOR 5th Percentile Female NHTSA Advanced Frontal Dummy. 2017, National Highway Traffic Safety Administration: Washington, DC, USA. p. 54.

[41] Forman, J., Ruyun, J., Östling, M., and Jeppsson, H. Collision, occupant, and injury characteristics in low-to-moderate speed frontal collisions – an examination of U.S. field data from 2017-2022, in *Proceedings of the IRCOBI Conference 2025*. 2025: Vilnius, Lithuania.

[42] Assessment Protocol - Adult Occupant Protection. 2023, European New Car Assessment Programme (Euro NCAP).

[43] Wang, S.C., Brede, C., et al. Gender differences in hip anatomy: possible implications for injury tolerance in frontal collisions. *Annual proceedings. Association for the Advancement of Automotive Medicine*, 2004. 48: p. 287-301

[44] Jones, M.L.H., Ebert, S.M., et al. Effect of Class I-III obesity on driver seat belt fit. *Traffic Inj Prev*, 2021. 22(7): p. 547-552

[45] Brumbelow, M.L. Female Driver Lower Extremity Injury: Contributing Factors and Crash Test Relevance. *Proceedings of International Research Council on the Biomechanics of Injury (IRCOBI)*, 2023. Cambridge, UK

[46] Chang, C.Y., Rupp, J.D., Reed, M.P., Hughes, R.E., and Schneider, L.W. Predicting the effects of muscle activation on knee, thigh, and hip injuries in frontal crashes using a finite-element model with muscle forces from subject testing and musculoskeletal modeling. *Stapp Car Crash J*, 2009. 53: p. 291-328

[47] Filatov, A., Scanlon, J.M., Bruno, A., Danthurthi, S.S.K., and Fisher, J. Effects of Innovation in Automated Vehicles on Occupant Compartment Designs, Evaluation, and Safety: A Review of Public Marketing, Literature, and Standards. 2019.

VIII. APPENDIX

Appendix A: Generalized Female PMHS Lumped Parameter Model

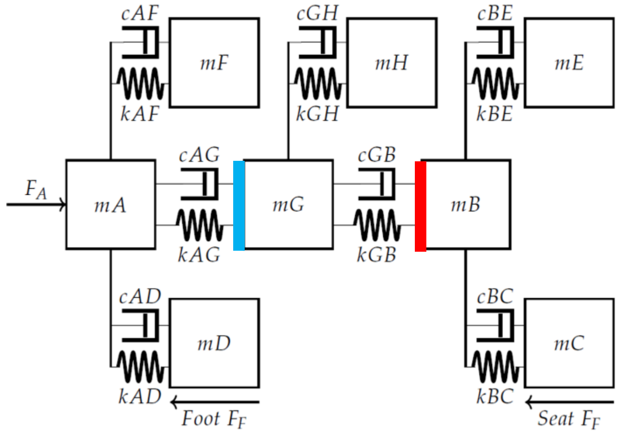

Fig. A1. Analytical model used to characterize force transfer along the KTH complex. Femur force calculation location is noted in blue, and hip force calculation location is noted in red. Variables correspond to different KTH regions and include masses, stiffness, damping, and frictional interactions. mA is the mass of the distal femur, knee, and surrounding knee flesh; mB is the mass of the pelvis; mC is the mass of the pelvis flesh; mD is the mass below the knee; mE is the upper body mass; mF is the distal thigh flesh; mG is the proximal femur; and mH is the proximal thigh flesh.

TABLE AI
GENERALIZED FEMALE MODEL VALUES

Model Parameter	Generalized Female PMHS	PMHS 1 [37]	PMHS 2 [37]	PMHS 3 [37]	PMHS 4 [37]
mA	1.09 kg	1.180 kg	1.009 kg	1.288 kg	0.886 kg
mB	0.65 kg	0.742 kg	0.626 kg	0.576 kg	0.650 kg
mC	5.50 kg	4.527 kg	6.725 kg	5.916 kg	4.815 kg
mD	2.17 kg	1.879 kg	2.218 kg	2.830 kg	1.746 kg
mE	10.77 kg	10.659 kg	12.927 kg	10.885 kg	8.618 kg
mF	1.30 kg	1.121 kg	1.745 kg	1.486 kg	0.846 kg
mG	0.28 kg	0.273 kg	0.301 kg	0.263 kg	0.294 kg
mH	1.30 kg	1.121 kg	1.745 kg	1.486 kg	0.846 kg
kAG	452,209 N/m	457768 N/m	572456 N/m	441384 N/m	490536 N/m
cAG	2,494 Ns/m	2364 Ns/m	4316 Ns/m	5340 Ns/m	1468 Ns/m
kGB	192,630 N/m	444120 N/m	38616 N/m	661208 N/m	259800 N/m
cGB	2,254 Ns/m	1904 Ns/m	3120 Ns/m	976 Ns/m	1040 Ns/m
kBC	165,856 N/m	141034 N/m	187114 N/m	88810 N/m	3050 N/m
cBC	1,541 Ns/m	1184 Ns/m	1080 Ns/m	1064 Ns/m	2616 Ns/m
kAD	11 N/m	15 N/m	15 N/m	15 N/m	11 N/m
cAD	222 Ns/m	195 Ns/m	220 Ns/m	204 Ns/m	236 Ns/m
kBE	11 N/m	7 N/m	7 N/m	7 N/m	15 N/m
cBE	69 Ns/m	203 Ns/m	155 Ns/m	34 Ns/m	29 Ns/m
kAF	73,105 N/m	62654 N/m	101566 N/m	48318 N/m	59582 N/m
cAF	153 Ns/m	116 Ns/m	212 Ns/m	148 Ns/m	108 Ns/m
kGH	73,105 N/m	62654 N/m	101566 N/m	48318 N/m	59582 N/m
cGH	153 Ns/m	116 Ns/m	212 Ns/m	148 Ns/m	108 Ns/m

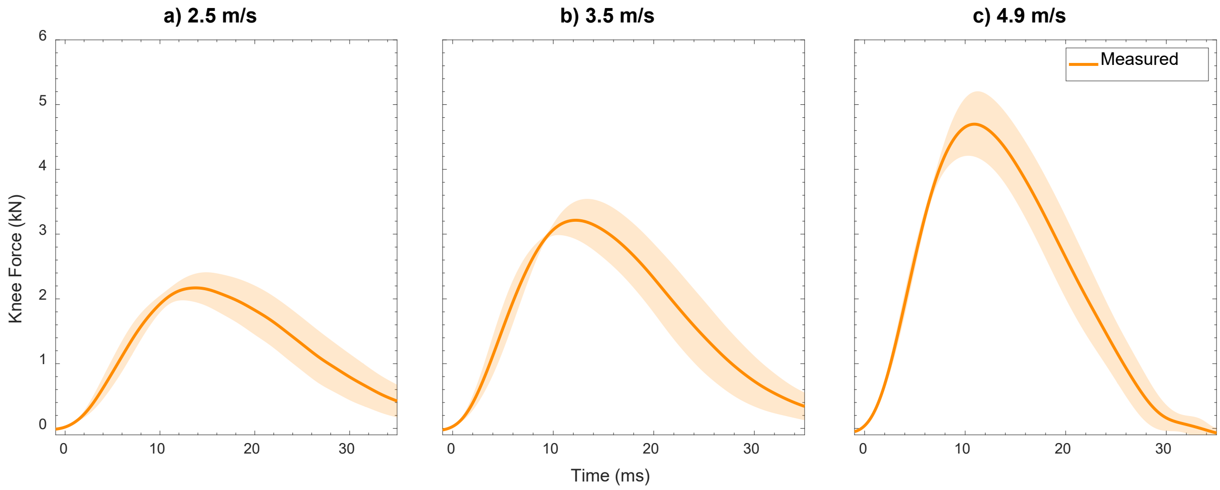

Fig. A2. Average Knee force measured for the four female PMHS (± one standard deviation) at impact velocities of (a) 2.5 m/s, (b) 3.5 m/s, and (c) 4.9 m/s. Positive axial force is directed along the length of the femur, loading it in compression.

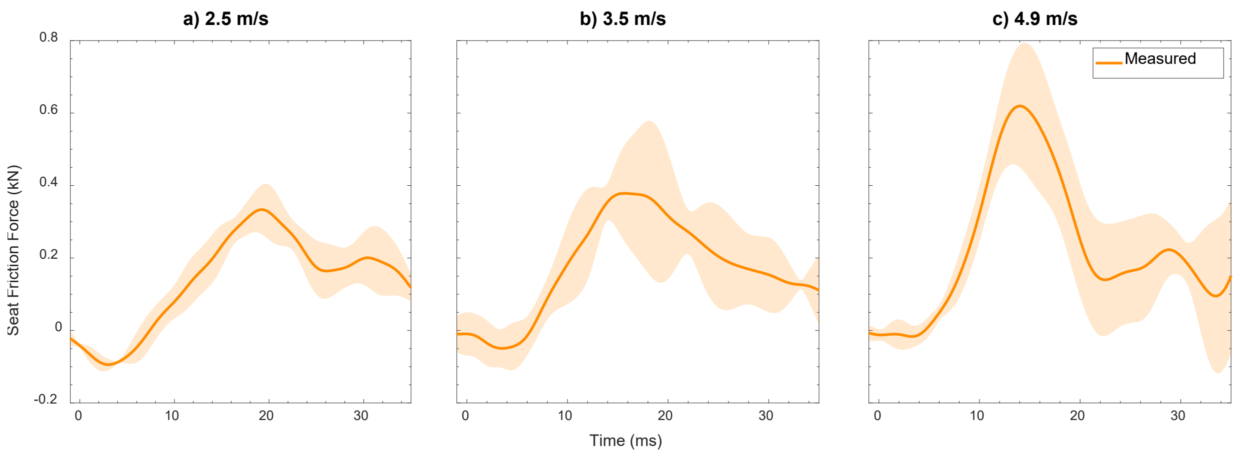

Fig. A3. Average seat friction force for the four female PMHS (± one standard deviation) at impact velocities of (a) 2.5 m/s, (b) 3.5 m/s, and (c) 4.9 m/s. Positive values indicate shearing of the seat plate along the principal direction of motion.

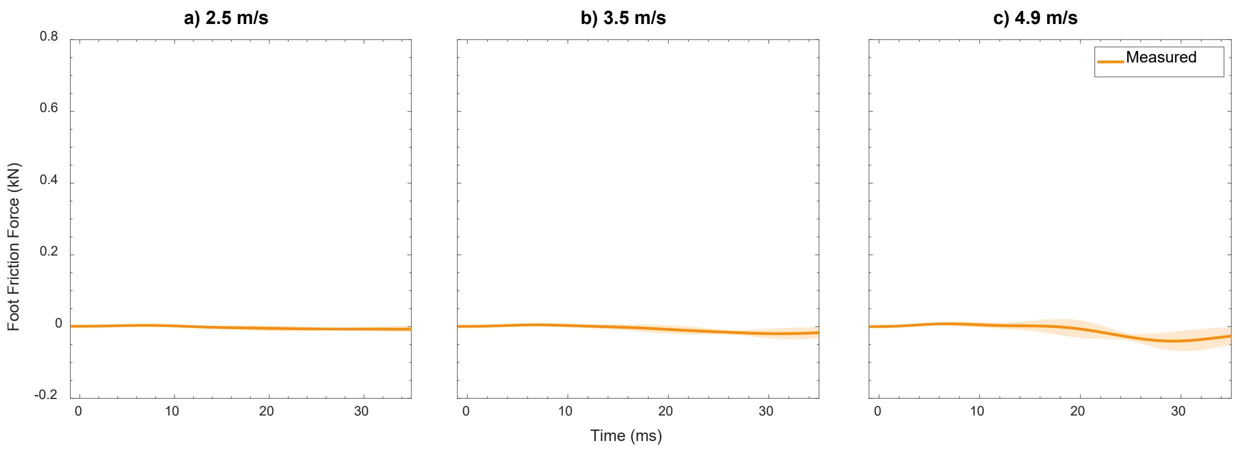

Fig. A4. Average foot friction force for the four female PMHS (± one standard deviation) at impact velocities of (a) 2.5 m/s, (b) 3.5 m/s, and (c) 4.9 m/s. Positive values indicate shearing of the foot plate along the principal direction of motion.

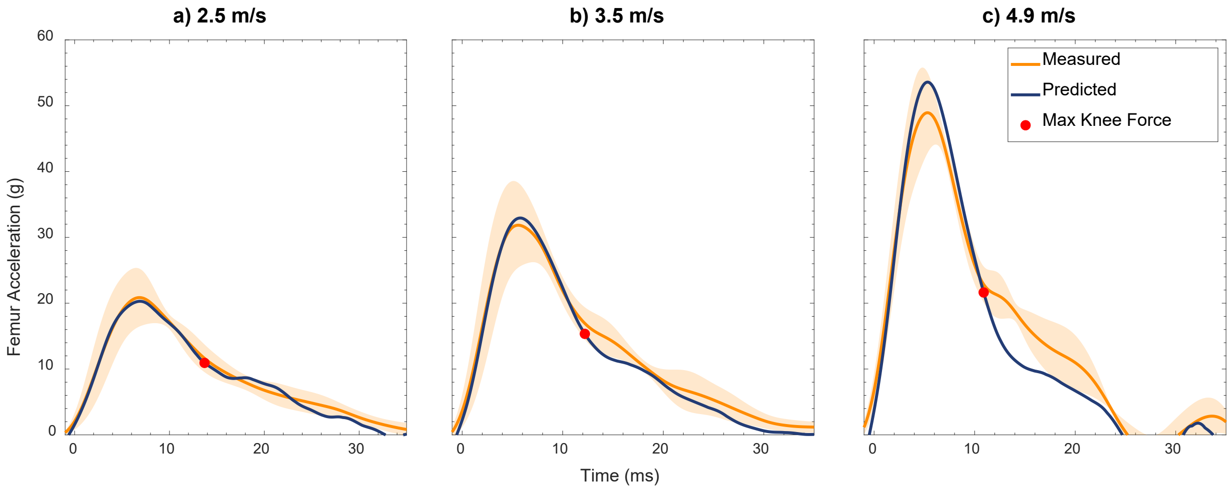

Fig. A5. Comparison of model-predicted distal femur acceleration to the average measured distal femur acceleration for the four whole-body female PMHS (± one standard deviation) at impact velocities of (a) 2.5 m/s, (b) 3.5 m/s, and (c) 4.9 m/s. Positive acceleration indicates anterior to posterior femur motion. Note: Maximum knee force is overlayed to show model performance up to this value, all within one standard deviation of the responses.

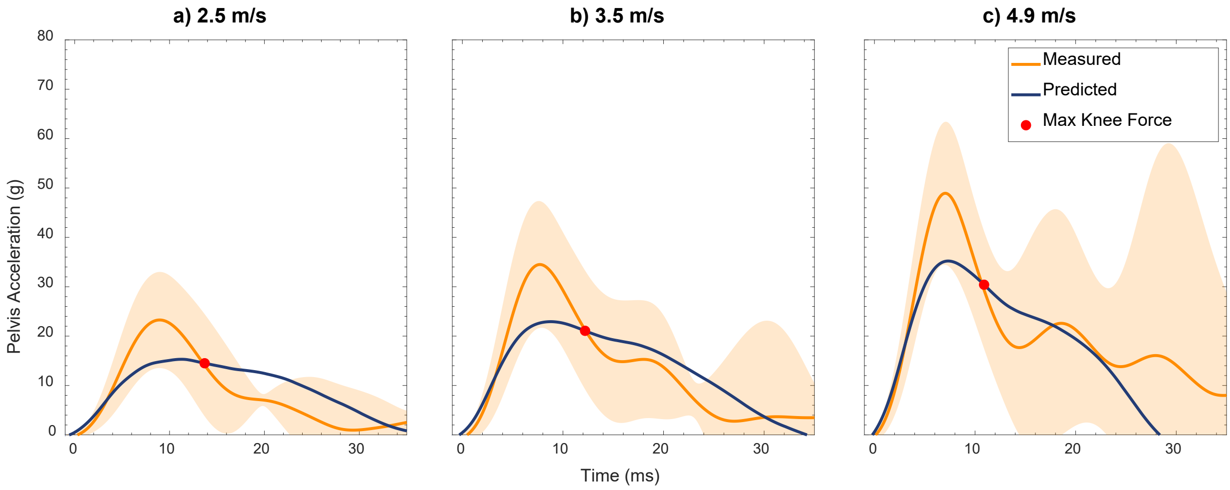

Fig. A6. Comparison of model-predicted pelvis acceleration to the average measured pelvis acceleration for four whole-body female PMHS (± one standard deviation) at impact velocities of (a) 2.5 m/s, (b) 3.5 m/s, and (c) 4.9 m/s. Positive acceleration indicates anterior to posterior pelvis motion. Note: Maximum knee force is overlayed to show model performance up to this value, all within one standard deviation of the responses.

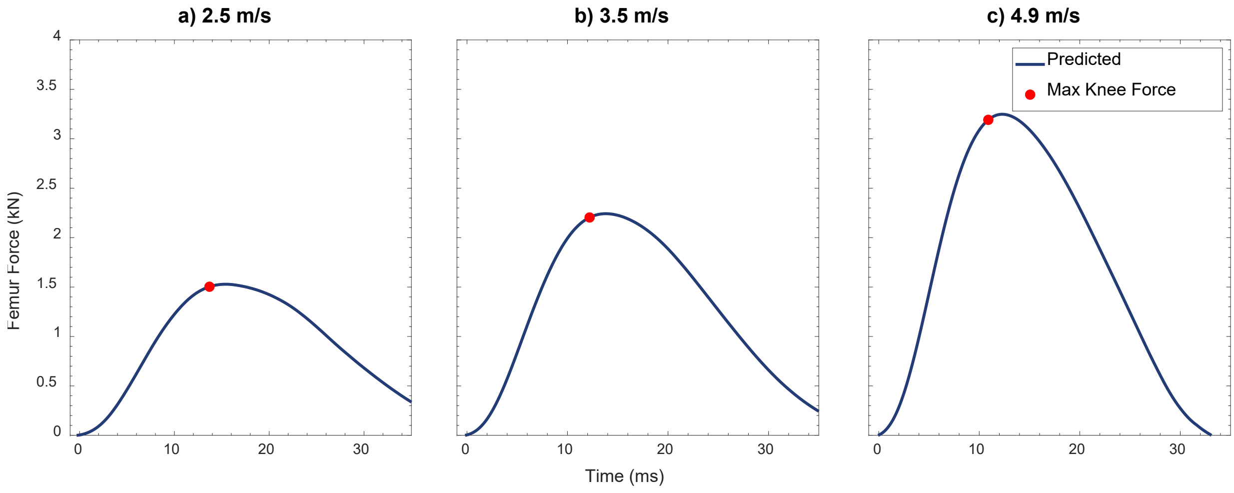

Fig. A7. Model-predicted femur force for the generalized female PMHS model at impact velocities of (a) 2.5 m/s, (b) 3.5 m/s, and (c) 4.9 m/s. Positive axial femur force is directed along the length of the femur, loading it in compression.

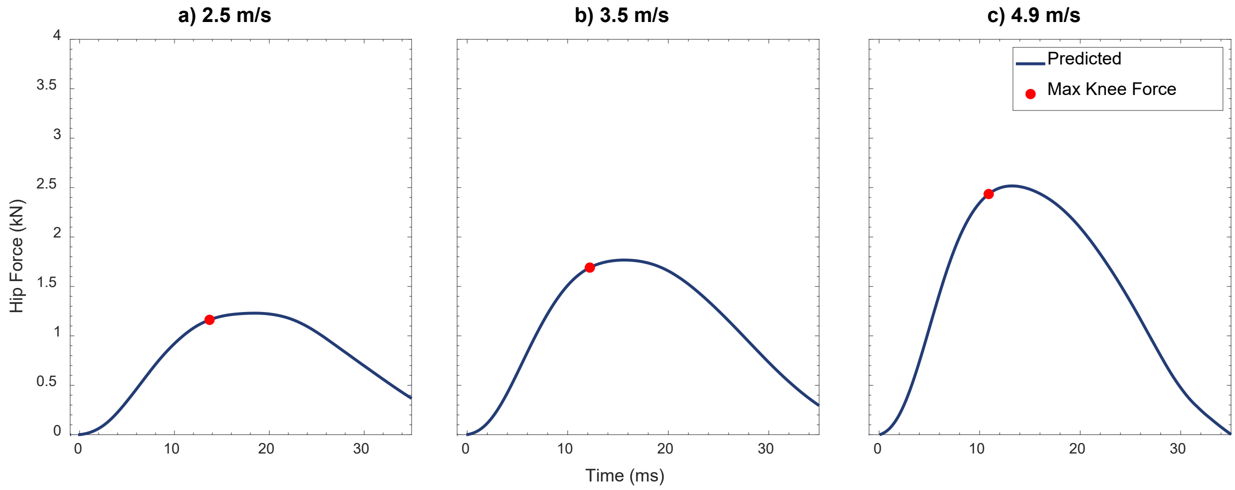

Fig. A8. Model-predicted hip force for the generalized female PMHS model at impact velocities of (a) 2.5 m/s, (b) 3.5 m/s, and (c) 4.9 m/s. Positive hip force indicates a force from the femur directed into the hip socket in the anterior-to-posterior direction.

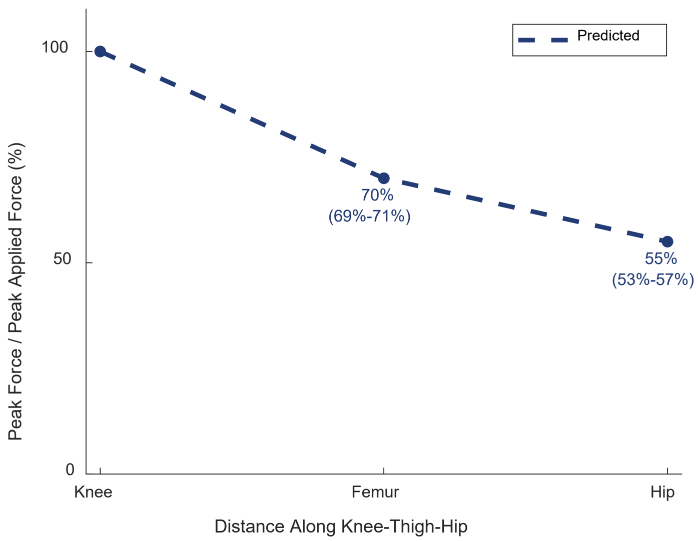

Fig. A9. Model-predicted KTH force transfer relationship for the generalized female PMHS model across all whole-body impacts.

Appendix B: THOR-05F Lumped Parameter Model Validation

TABLE BI
THOR-05F ATD MODEL

Model Parameter	Value	Description
mA	0.84 kg	½ mass of femur load cell and mass of knee and distal femur
mB	3.41 kg	Mass of the pelvis and pelvis flesh
mC	0.001 kg	Mass of the pelvis flesh (assumed rigidly affixed per [8])
mD	1.22 kg	Effective mass below the knee determined via optimization
mE	0.95 kg	Effective mass of the upper body, determined via optimization
mF	0.3 kg	Mass of the knee flesh
mG	3.49 kg	½ the mass of the femur load cell and mass of the remaining femur
mH	1.28 kg	Mass of the thigh flesh
kAG	1,013,800 N/m	Tuned coupling effect between the proximal and distal femur
cAG	4,000 Ns/m	
kGB	249,000 N/m	Tuned coupling effect between the proximal femur and hip
cGB	2,300 Ns/m	
kBC	1,000,000 N/m	Set to high values so the coupling is rigid [8]
cBC	25,000 Ns/m	
kAD	15,800 N/m	Tuned coupling effect between the lower leg and knee/distal femur
cAD	1,300 Ns/m	
kBE	1,100 N/m	Tuned coupling effect between the pelvis and upper body
cBE	300 Ns/m	
kAF	1,000,000 N/m	Set to high values so the coupling is rigid [8]
cAF	25,000 Ns/m	
kGH	1,000,000 N/m	Set to high values so the coupling is rigid [8]
cGH	25,000 Ns/m	

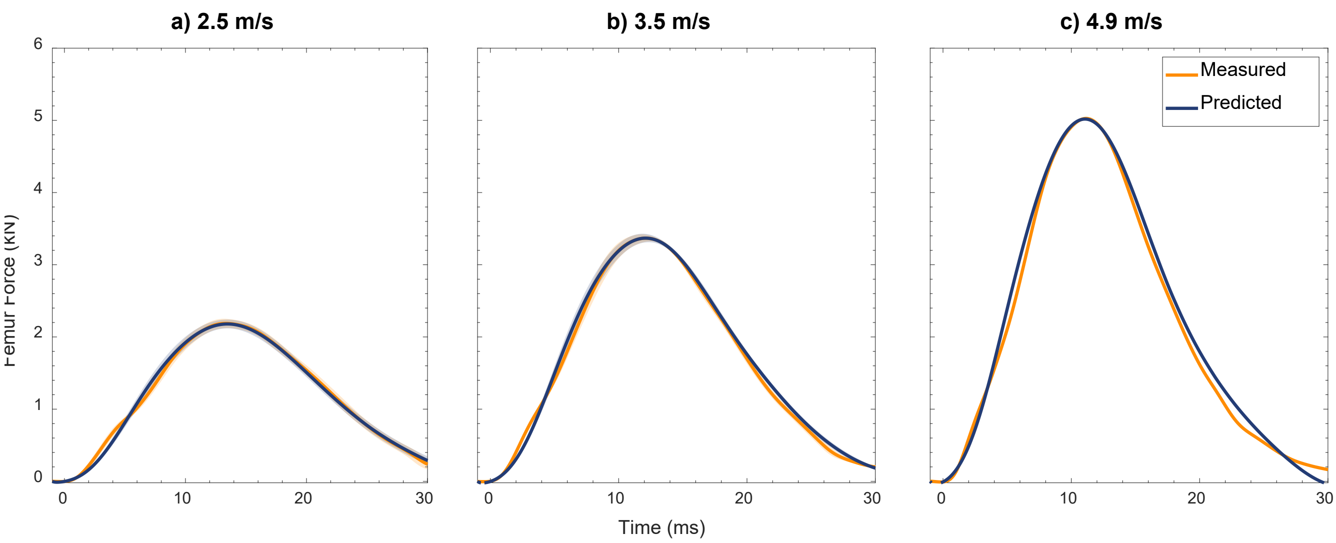

Fig. B1. Average femur axial force measured/predicted for THOR-05F (± one standard deviation) at impact velocities of (a) 2.5 m/s, (b) 3.5 m/s, and (c) 4.9 m/s. Positive axial force is directed along the length of the femur, loading it in compression. Note: There is no standard deviation bar for the 4.9 m/s impacts as only one test was conducted at this velocity.

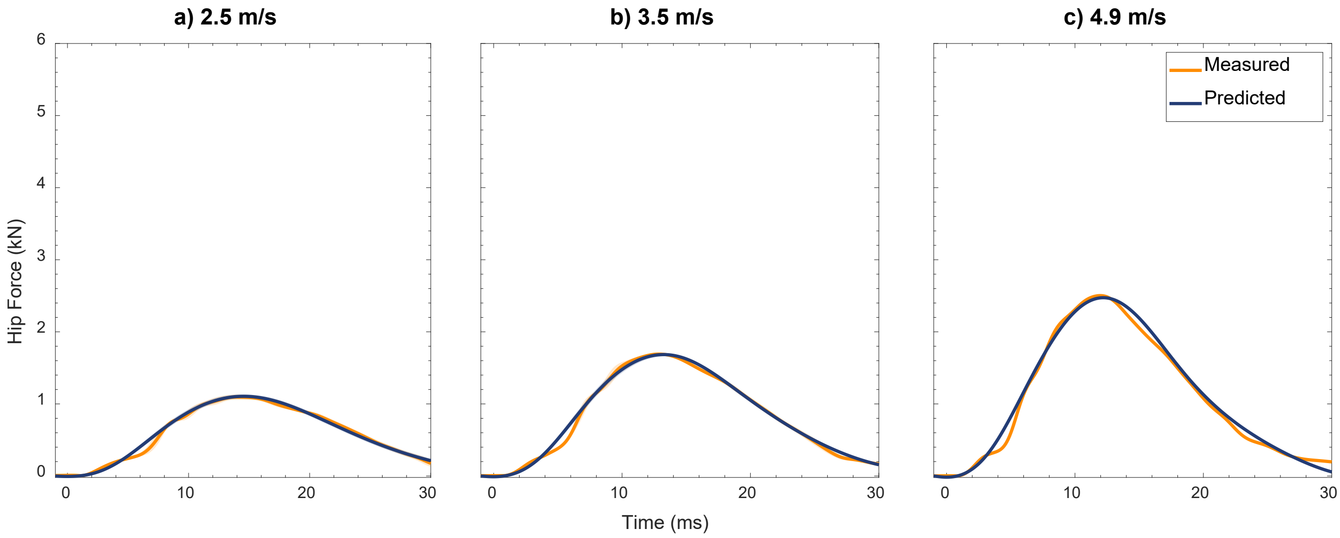

Fig. B2. Average resultant hip force measured/predicted for THOR-05F (± one standard deviation) at impact velocities of (a) 2.5 m/s, (b) 3.5 m/s, and (c) 4.9 m/s. Positive hip force is directed into the acetabulum, loading the pelvis in the anterior-posterior (A-P) direction. Note: There is no standard deviation bar for the 4.9 m/s impacts as only one test was conducted at this velocity.

TABLE BII
THOR-05F MODEL VALIDATION FEMUR

Impact Velocity (m/s)	Type	Time to Maximum Force (s)	Impulse of Loading (Ns)	Force Transfer Percentage (%)
	Measured	0.0133	36.81	83.07
2.5	Predicted	0.0135	36.76	82.78
	Error (%)	1.50	0.14	0.35
	Measured	0.0121	50.04	82.45
3.5	Predicted	0.0121	51.09	82.46
	Error (%)	0.00	2.10	0.01
	Measured	0.0111	64.49	82.46
4.9	Predicted	0.0111	67.2	82.32
	Error (%)	0.00	4.20	0.17

TABLE BIII
THOR-05F MODEL VALIDATION HIP

Impact Velocity (m/s)	Type	Time to Maximum Force (s)	Impulse of Loading (Ns)	Force Transfer Percentage (%)
	Measured	0.0141	18.60	41.56
2.5	Predicted	0.0146	18.86	41.99
	Error (%)	3.55	1.40	1.03
	Measured	0.0129	25.39	41.39
3.5	Predicted	0.0132	25.84	41.24
	Error (%)	2.33	1.77	0.36
	Measured	0.012	32.51	41.05
4.9	Predicted	0.0122	33.65	40.57
	Error (%)	1.67	3.51	1.17

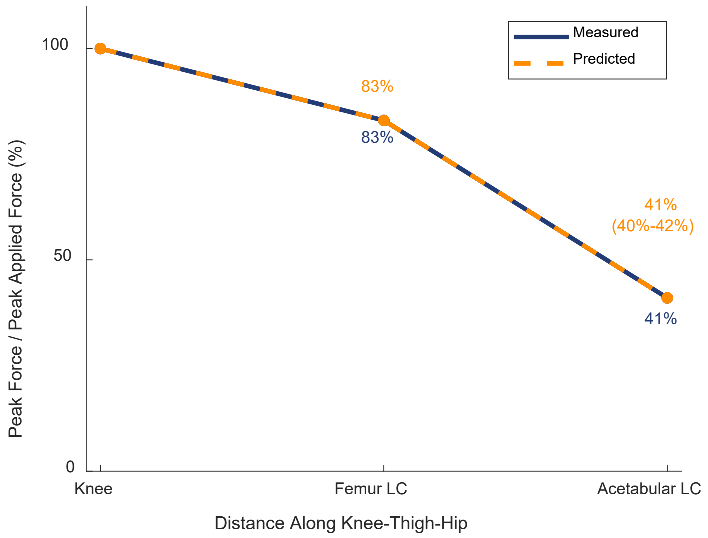

Fig. B3. Average knee-thigh-hip force transfer (± one standard deviation when noted) for the THOR-05F, measured experimentally and compared to model predictions. The values were calculated by dividing the maximum femur and hip forces (both experimental and model-derived) by the maximum applied force, then converting these ratios to percentages.

Appendix C: Theoretical Knee Bolster Simulations

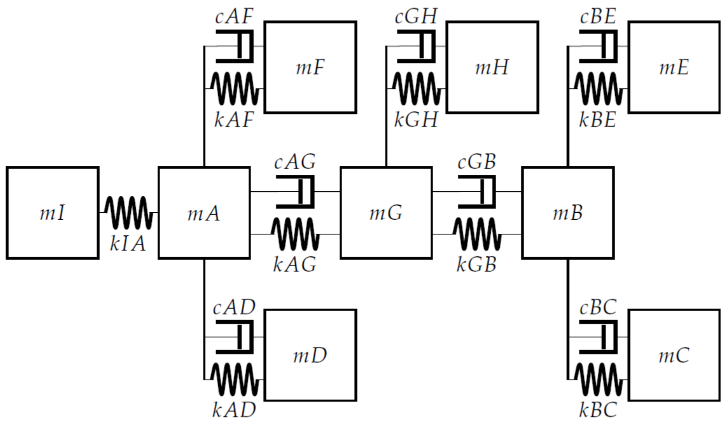

Fig. C1. Updated lumped parameter model developed to characterize the force transfer along knee-thigh-hip under loading conditions not explored with the experimental testing and defined previously by [8].

TABLE CI
BOLSTER PARAMETER THEORY USED FOR ANALYSIS

Bolster Type	Sample Force-Deformation Profile	Governing Equation(s) for Bolster Force	Simulation Parameters [8]
Linear Force-Deflection	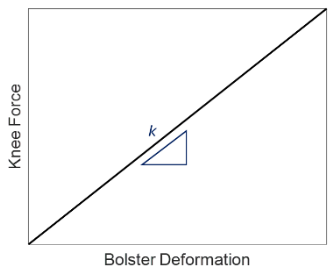	The calculation for bolster force is derived from Hooke's law, represented by: $F = kx$	1. *Bolster Stiffness*: 50-450 N/mm 2. *Impact Velocity*: 2-8 m/s

Bilinear Force-Deflection	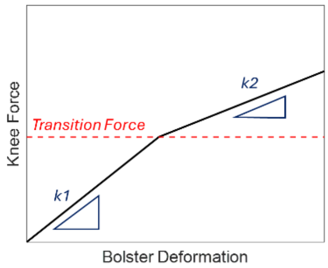	Prior to the transition force, the calculation is equivalent to the linear case. After the transition force: $F = k_2x + (k_1 - k_2)x_{trans}$, where k_1 is the initial stiffness, k_2 is the secondary stiffness, and x_{trans} is the bolster deformation at transition.	1. *Bolster Stiffness*: 50-450 N/mm 2. *Transition Force*: 2-8 kN 3. *Secondary Stiffness*: 50-250 N/mm 4. *Impact Velocity*: 2-8 m/s
Force Limiting	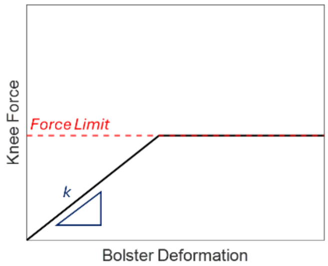	The force limiting bolster is a special case of the bilinear bolster, with the force limit replacing the transition force, and $k_2 = 0\ N/mm$	1. *Bolster Stiffness*: 200-450 N/mm 2. *Impact Velocity*: 3-8 m/s 3. *Force Limit*: 4-18 kN

TABLE CII

SMALL FEMALE MODEL PARAMETERS USED FOR SIMULATIONS

Model Parameter	Hybrid III [36]	THOR	Female PMHS
mA	1.75 kg	0.84 kg	1.09 kg
mB	4.48 kg	3.41 kg	0.65 kg
mC	0.001 kg	0.001 kg	5.50 kg
mD	0.32 kg	1.22 kg	2.17 kg
mE	3.41 kg	0.95 kg	10.77 kg
mF	0.57 kg	0.3 kg	1.30 kg
mG	2.46 kg	3.49 kg	0.28 kg
mH	0.001 kg	1.28 kg	1.30 kg
kAG	3,000,000 N/m	1,013,800 N/m	452,209 N/m
cAG	25,000 Ns/m	4,000 Ns/m	2,494 Ns/m
kGB	3,000,000 N/m	249,000 N/m	192,630 N/m
cGB	30,000 Ns/m	2,300 Ns/m	2,254 Ns/m
kBC	1,000,000 N/m	1,000,000 N/m	165,856 N/m
cBC	25,000 Ns/m	25,000 Ns/m	1,541 Ns/m
kAD	13,520 N/m	15,800 N/m	11 N/m
cAD	1,000 Ns/m	1,300 Ns/m	222 Ns/m
kBE	500 N/m	1,100 N/m	11 N/m
cBE	1,500 Ns/m	300 Ns/m	69 Ns/m
kAF	1,000,000 N/m	1,000,000 N/m	73,105 N/m
cAF	25,000 Ns/m	25,000 Ns/m	153 Ns/m
kGH	1,000,000 N/m	1,000,000 N/m	73,105 N/m
cGH	25,000 Ns/m	25,000 Ns/m	153 Ns/m

PMHS Simulation Results:

TABLE CIII
SMALL FEMALE MODEL SIMULATION RESULTS (LOADING PERCENTILES)

	Knee		*Femur*		*Hip*	
Percentile	*Peak Force (kN)*	*Loading Rate (N/ms)*	*Peak Force (kN)*	*Loading Rate (N/ms)*	*Peak Force (kN)*	*Loading Rate (N/ms)*
5	2.78	264	1.94	176	1.52	114
25	4.45	522	3.09	331	2.48	206
50	5.79	804	4.05	501	3.23	321
75	7.14	1186	4.98	717	3.96	484
95	8.69	1914	5.98	1062	4.67	796

Hybrid III Simulation Results:

TABLE CIV
HYBRID III SMALL FEMALE MODEL SIMULATION RESULTS (LOADING PERCENTILES)

	Knee		*Femur Load Cell*	
Percentile	*Peak Force (kN)*	*Loading Rate (N/ms)*	*Peak Force (kN)*	*Loading Rate (N/ms)*
5	3.71	315	2.96	252
25	5.58	629	4.46	499
50	7.50	974	6.00	767
75	9.44	1412	7.54	1101
95	12.39	2281	9.88	1756

THOR Simulation Results:

TABLE CV
THOR SMALL FEMALE MODEL SIMULATION RESULTS (LOADING PERCENTILES)

	Knee		*Femur Load Cell*		*Acetabular Load Cell*	
Percentile	*Peak Force (kN)*	*Loading Rate (N/ms)*	*Peak Force (kN)*	*Loading Rate (N/ms)*	*Peak Force (kN)*	*Loading Rate (N/ms)*
5	3.36	304	2.73	256	1.34	126
25	5.14	604	4.18	501	2.05	239
50	6.83	929	5.56	761	2.73	355
75	8.50	1348	6.97	1083	3.42	483
95	11.00	2122	8.98	1643	4.39	681

Knee Bolster Penetration Simulation Results:

TABLE CVI
SMALL FEMALE MODEL SIMULATION RESULTS (KNEE BOLSTER PENETRATION COMPARISON)

Percentile	*PMHS Penetration (mm)*	*Hybrid III Penetration (mm)*	*THOR Penetration (mm)*
5	10.0	16.1	13.7
25	17.6	27.5	23.6
50	25.5	38.7	33.3
75	36.4	51.0	44.7
95	60.6	74.9	67.8

Appendix D: Small Female IRFs and IARVs

Small Female KTH Injury Risk Function Definitions: A summary of the IRFs used for to define a small female is shown in table D1. It is important to note that the IRFs use cadaver force inputs from different locations along KTH, and thus interpreting KTH IRFs from the wrong location leads to inaccurate injury assessments. For example, the knee/distal femur IRF relates the applied force at the cadaver knee to knee/distal femur injury risk. In cases where the applied knee force cannot be measured, estimates of knee/femur injury risk from femur loads will underpredict injury risk without accounting for the force drop from the knee to the femur. In this study, knee impact tests and analytical simulations showed that knee-to-femur force transmission was consistently around 70% on average. To express the knee/distal femur IRFs in terms of midshaft femur force for small female simulations, a femur-to-knee correction factor (T_{Knee}) of 1.43 (1/0.70) is thus required. Further, due to similar force transmission behaviour across test series [8], this correction factor is also likely reasonable for midsize male simulations. To further investigate, the current setup can be replicated using a finite element model to determine if the 70% value holds.

TABLE DI

SMALL FEMALE INJURY RISK FUNCTION DEFINITIONS

Function	*Input*	*Output*	*Assumptions*
$p(AIS\ 2+) = \Phi\left[\frac{Ln[F_{\max_{knee}}] - 2.224}{0.3014}\right]$	Maximum applied knee force ($F_{\max_{knee}}$)	Probability of knee/distal femur AIS 2+ injuries	Recommended IRF from [1], assuming a female (♂=0)
$p(Hip\ FX) = \Phi\left[\frac{Ln\left[F_{\max_{hip}}\right] - 1.309}{0.2339}\right]$	Maximum hip force ($F_{\max_{Hip}}$)	Probability of hip fracture or dislocation	Recommended IRF from [1], assuming a small female (stature = 150 cm, hip flexion angle = 15°)

Small Female KTH Injury Assessment Reference Value Definitions: Using Table D1 above, a set of KTH IARVs for the small female can be extracted from the IRFs, corresponding to injury risks of 3%, 5%, 10%, 15%, 25%, 30%, 35%, 40%, 45%, 50%, and 75% which have been used previously [8] (Table D2). The ATD correction factors developed were then applied to these values as discussed below.

TABLE DII

SMALL FEMALE INJURY ASSESSMENT REFERENCE VALUES

Measurement	*Applied Knee Force*	*Hip Force*
Risk (%)	*Knee/Distal Femur IRF ($T_{Knee} = 1$)*	*Hip IRF ($T_{Hip} = 1$)*
3	5.24	2.38
5	5.63	2.52
10	6.28	2.74
15	6.76	2.91
20	7.17	3.04
25	7.54	3.16
30	7.89	3.28
35	8.23	3.38
40	8.56	3.49
45	8.90	3.60
50	9.24	3.70
75	11.33	4.34

Commentary on Differences Between IRFs: The two KTH IRFs used throughout this study generally estimate a higher risk of hip injury compared to knee/distal femur injury. This trend forms the basis for the lower and upper force limits, as shown in Fig. D1. For a higher maximum risk of knee/distal femur injury to be predicted under the current IRFs, the knee-to-hip force transfer ratio for the PMHS would need to be less than 45%, which did not occur in either the simulated or measured impacts. This is further highlighted in Fig. D2, as the estimated hip injury risk across the simulation parameters for the generalized small female PMHS model consistently predicted a higher risk of hip injury throughout the tests, shown by the analytical simulations generally falling above the black dotted line (which represents equal knee/distal femur and hip injury risk estimations).

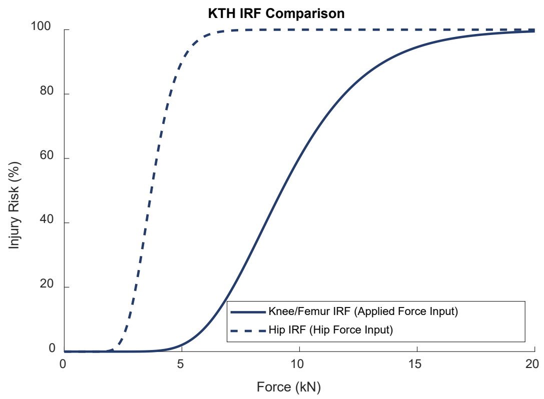

Fig. D1. Comparison of the cadaver-based Knee/Distal Femur and the Hip IRFs used in this study, using the assumptions from Table D1.

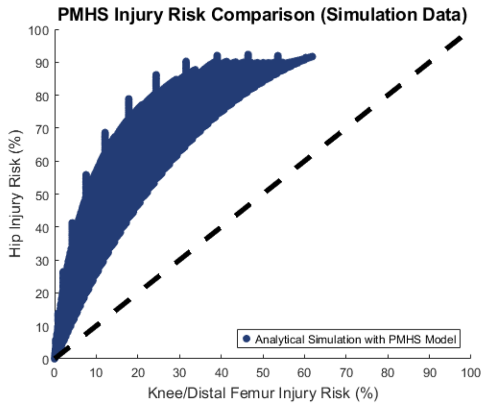

Fig. D2. Comparison of the Knee/Distal Femur and the Hip injury risk predicted using the results of the analytical simulation data.

Experimentally Observed Correction Factors (Female): Using the results from previous small female experimental knee impact tests from [36,37] and the small female generalized model knee-to-hip force transfer estimations under the experimental conditions, a set of KTH force transfer relationships were determined by normalizing each subject's force transfer relative to the PMHS applied knee force. Using these relationships, experimental correction factors were then established. Inputting these values from Table 1 yields Eq. D1-D3 for the hip (relative to each load cell):

$$T_{\frac{hip}{H3}} = \frac{r_{KH_{PMHS}}}{r_{KT_{H3}}} = \frac{0.55}{1.09} = 0.50 \qquad (D1)$$

$$T_{\frac{hip}{THOR_{Fem}}} = \frac{r_{KH_{PMHS}}}{r_{KT_{THOR}}} = \frac{0.55}{1.03} = 0.53 \qquad (D2)$$

$$T_{\frac{hip}{THOR_{Acet}}} = \frac{r_{KH_{PMHS}}}{r_{KH_{THOR}}} = \frac{0.55}{0.52} = 1.06 \qquad (D3)$$

Similarly, for use with the knee/distal femur IRF (Eq. D4-D6):

$$T_{\frac{Knee}{H3}} = \frac{1}{r_{KT_{H3}}} = \frac{1}{1.09} = 0.92 \qquad (D4)$$

$$T_{\frac{Knee}{THOR_{Fem}}} = \frac{1}{r_{KT_{THOR}}} = \frac{1}{1.03} = 0.97 \qquad (D5)$$

$$T_{\frac{Knee}{THOR_{Acet}}} = \frac{1}{r_{KH_{THOR}}} = \frac{1}{0.52} = 1.92 \qquad (D6)$$

Small Female ATD Hip IRFs (Experimental Assumption): Applying T_{Hip} to the hip IRF in Eq. 2 yields Eq. D7 for the Hybrid III femur load cell and Eq. D8 and Eq. D9 for the THOR-05F load cells:

$$p_{H3}(Hip\ FX) = \Phi\left[\frac{Ln\left[0.50 * F_{Fem\ LC_{max}}\right] - 1.309}{0.2339}\right] \qquad (D7)$$

$$p_{THOR_{Fem}}(Hip\ FX) = \Phi\left[\frac{Ln\left[0.53 * F_{Fem\ LC_{max}}\right] - 1.309}{0.2339}\right] \qquad (D8)$$

$$p_{THOR_{Acet}}(Hip\ FX) = \Phi\left[\frac{Ln\left[1.06 * F_{Acet\ LC_{max}}\right] - 1.309}{0.2339}\right] \qquad (D9)$$

These IRFs are expressed visually in Fig. D3 relative to the original PMHS Hip IRF. Under the experimental conditions, both ATD femur load cells were approximately double the magnitude of the PMHS hip force, so they are shifted to the right of the original Hip IRF. Conversely, the THOR acetabular load cell was slightly less than the

PMHS hip force under the experimental conditions, so this IRF has been shifted slightly to the left of the original Hip IRF.

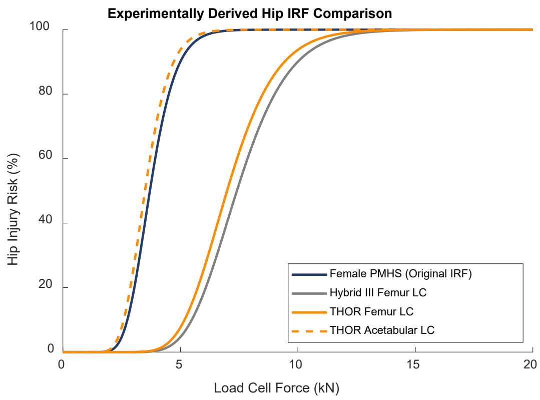

Fig. D3. Comparison of the cadaver-based Hip IRF used in this study to the ATD IRFs derived using the unique T_{Hip} correction factor for each ATD load cell derived from the experimental knee impact force transfer relationships.

Small Female ATD Knee/Distal Femur IRFs (Experimental Assumption): Similarly, applying T_{Knee} to the knee/distal femur IRF in Eq. 1 yields Eq. D10 for the Hybrid III femur load cell and Eq. D11 and Eq. D12 for the THOR-05F load cells:

$$p_{H3}(Knee/Distal\ Femur\ AIS\ 2+) = \Phi\left[\frac{Ln\left[0.92 * F_{Fem\ LC_{max}}\right] - 2.224}{0.3014}\right] \quad (D10)$$

$$p_{THOR_{Fem}}(Knee/Distal\ Femur\ AIS\ 2+) = \Phi\left[\frac{Ln\left[0.97 * F_{Fem\ LC_{max}}\right] - 2.224}{0.3014}\right] \quad (D11)$$

$$p_{THOR_{Acet}}(Knee/Distal\ Femur\ AIS\ 2+) = \Phi\left[\frac{Ln\left[1.92 * F_{Acet\ LC_{max}}\right] - 2.224}{0.3014}\right] \quad (D12)$$

These IRFs are expressed visually in Fig. D4 relative to the original PMHS Knee/Distal Femur IRF. Under the experimental conditions, both ATD femur load cells were slightly greater in magnitude compared to the PMHS knee force, so they are shifted slightly to the right of the original Knee/Distal Femur IRF. Conversely, the THOR acetabular load cell was less than the PMHS knee force under the experimental conditions, so this IRF has been shifted to the left of the original Knee/Distal Femur Hip IRF.

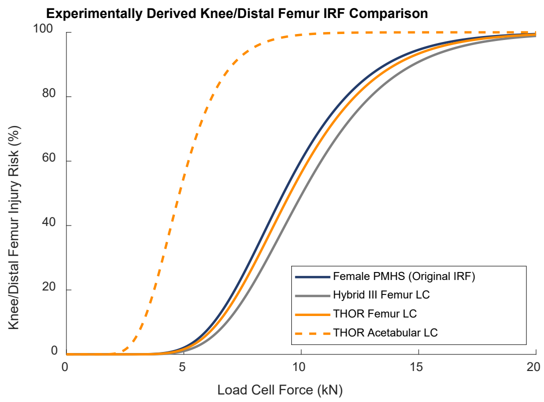

Fig. D4. Comparison of the cadaver-based Knee/Distal Femur IRF used in this study to the ATD IRFs derived using the unique T_{Knee} correction factor for each ATD load cell derived from the experimental knee impact force transfer relationships.

Appendix E: IARB Derivations

Small Female Transition Force Derivation: To adapt the KTH transition force in the IARB method for small female ATDs, the 2.89 kN value used for the midsize male was scaled using previously established methodologies for translating forces from the midsize male to small female. These are shown in Eq. E1 below, derived from assuming a constant density relationship:

$$\lambda_{Force} = \lambda_k \lambda_z = \left(\frac{\lambda_x^2}{\lambda_z}\right)\lambda_z = \lambda_x^2 = 0.79 \quad (E1)$$

This was then used to obtain a scaled lowest hip fracture force of the small female of 2.28 kN obtained from Eq. E2:

$$Force\ Limit\ for\ Impulse = 2.89\ kN * \lambda_{Force} = 2.89\ kN * 0.79 = 2.28\ kN \qquad (E2)$$

Which, when comparing this value to Table D2, is below all risk levels associated with the Hip IARVs.

<u>Conservative Impact Assumption Correction Factors (Male and Female):</u> The current correction factors for the midsize male, derived from the conservative impact assumption, are shown below for the Hybrid III femur load cells (Equation E3) and the THOR acetabular load cells (Equation E4) and includes the final transfer functions that have been used for the midsize males [1,8]. These values are then applied to the Hip IRF, by substituting the maximum force term (F_{max}), by the maximum load cell measurement in the ATD multiplied by the transfer function ($T_{Hip} * F_{LC_{max}}$).

$$T_{\frac{hip}{H3}} = \frac{r_{KH_{PMHS}}}{r_{KT_{H3}}} = \frac{0.55}{0.77} = 0.7143 = \frac{1}{1.4} \qquad (E3)$$

$$T_{\frac{hip}{THOR_{Acet}}} = \frac{r_{KH_{PMHS}}}{r_{KH_{THOR}}} = \frac{r_{KH_{PMHS}}}{r_{KT_{H3}} * r_{TH_{THOR}}} = \frac{0.55}{0.77 * 0.5} = 1.429 \qquad (E4)$$

Similarly, for use with the knee/distal femur IRF (Eq. E5):

$$T_{\frac{Knee}{H3}} = T_{\frac{Knee}{THOR_{Fem}}} = \frac{1}{r_{KT_{H3}}} = \frac{1}{0.77} = 1.3 \qquad (E5)$$

Note that, in the derivation of both correction factors, it was assumed that the knee-to-femur load cell behaviour was consistent across ATDs due to a lack of similar THOR data [1].

For application with the female ATDs, this methodology was adapted using the force transfer relationship determined from the results of the analytical simulations, normalized by each subject's maximum applied force at the knee. These assumptions are consistent with the midsize male ATD approach [1,8]. Inputting the values from Table 1 yields Eq. E6-E8 for the hip (relative to each load cell):

$$T_{\frac{hip}{H3}} = \frac{r_{KH_{PMHS}}}{r_{KT_{H3}}} = \frac{0.56}{0.80} = 0.70 = \frac{1}{1.43} \qquad (E6)$$

$$T_{\frac{hip}{THOR_{Fem}}} = \frac{r_{KH_{PMHS}}}{r_{KT_{THOR}}} = \frac{0.56}{0.81} = 0.69 = \frac{1}{1.45} \qquad (E7)$$

$$T_{\frac{hip}{THOR_{Acet}}} = \frac{r_{KH_{PMHS}}}{r_{KH_{THOR}}} = \frac{0.56}{0.40} = 1.40 \qquad (E8)$$

Similarly, for use with the knee/distal femur IRF (Eq. E9-E11):

$$T_{\frac{Knee}{H3}} = \frac{1}{r_{KT_{H3}}} = \frac{1}{0.80} = 1.25 \qquad (E9)$$

$$T_{\frac{Knee}{THOR_{Fem}}} = \frac{1}{r_{KT_{THOR}}} = \frac{1}{0.81} = 1.23 \qquad (E10)$$

$$T_{\frac{Knee}{THOR_{Acet}}} = \frac{1}{r_{KH_{THOR}}} = \frac{1}{0.4} = 2.50 \qquad (E11)$$

Looking at the work by [1], adapting the conservative correction factor approach of [8], yielded correction factors of 1.3 for T_{knee} (femur load cell) and 1.429 for T_{Hip} (acetabular load cell) for the THOR-50M. For the THOR-05F in this study, similar calculations yielded 1.23 for T_{knee} and 1.40 for T_{Hip}, which are consistent. In the original derivation, this ratio was assumed to be equivalent to the corresponding Hybrid III ratio ($r_{KT_{H3}}$) due to similarities in ATD construction up to the femur load cell and an absence of knee impact data for the THOR ATD [1,39]. The results of the current test series support the claim that the knee-to-femur load cell was consistent across ATDs. The values for $r_{KT_{THOR}}$ and $r_{KT_{H3}}$, obtained through the analytical simulation results, were nearly identical in value (0.81 and 0.80, respectively). The slight discrepancy between correction factors appears to arise from differences in $r_{KT_{THOR}}$, as the estimated force transmission is slightly higher than the 0.77 ratio originally assumed [1,8]. However, this difference was largely inconsequential as the resulting correction factors were still very close to one another, producing minimal differences in interpretation.

<u>Small Female ATD Hip IRFs (Lower Force Limit):</u> Applying T_{Hip} to the hip IRF in Eq. 2 yields Eq. E12 for the Hybrid III femur load cell and Eq. E13 and Eq. E14 for the THOR-05F load cells:

$$p_{H3}(Hip\ FX) = \Phi\left[\frac{Ln\left[0.7 * F_{Fem\ LC_{max}}\right] - 1.309}{0.2339}\right] \quad (E12)$$

$$p_{THOR_{Fem}}(Hip\ FX) = \Phi\left[\frac{Ln\left[0.69 * F_{Fem\ LC_{max}}\right] - 1.309}{0.2339}\right] \quad (E13)$$

$$p_{THOR_{Acet}}(Hip\ FX) = \Phi\left[\frac{Ln\left[1.40 * F_{Acet\ LC_{max}}\right] - 1.309}{0.2339}\right] \quad (E14)$$

These IRFs form the lower force limit for the small female IARBs in this study and are expressed visually in Fig. E1 relative to the original PMHS Hip IRF. Under force limiting conditions, both ATD femur load cells are greater in magnitude than the PMHS hip force, so they are to the right of the original Hip IRF. Conversely, the THOR acetabular load cell is less than the PMHS hip force under force limiting conditions, so this IRF has been shifted to the left of the original Hip IRF.

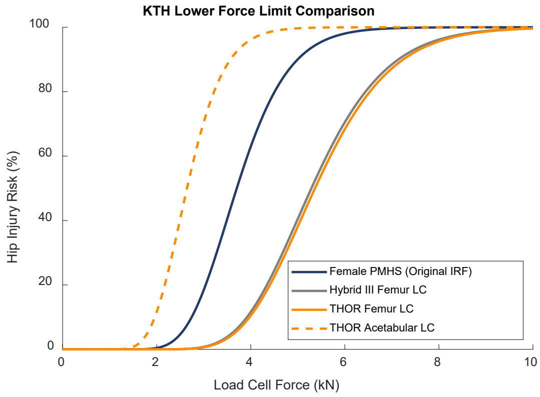

Fig. E1. Comparison of the cadaver-based Hip IRF used in this study to the ATD IRFs derived using the unique T_{Hip} correction factor for each ATD load cell.

Small Female ATD Knee/Distal Femur IRFs (Upper Force Limit): Similarly, applying T_{Knee} to the knee/distal femur IRF in Eq. 1 yields Eq. E15 for the Hybrid III femur load cell and Eq. E16 and Eq. E17 for the THOR-05F load cells:

$$p_{H3}(Knee/Distal\ Femur\ AIS\ 2+) = \Phi\left[\frac{Ln\left[1.25 * F_{Fem\ LC_{max}}\right] - 2.224}{0.3014}\right] \quad (E15)$$

$$p_{THOR_{Fem}}(Knee/Distal\ Femur\ AIS\ 2+) = \Phi\left[\frac{Ln\left[1.23 * F_{Fem\ LC_{max}}\right] - 2.224}{0.3014}\right] \quad (E16)$$

$$p_{THOR_{Acet}}(Knee/Distal\ Femur\ AIS\ 2+) = \Phi\left[\frac{Ln\left[2.50 * F_{Acet\ LC_{max}}\right] - 2.224}{0.3014}\right] \quad (E17)$$

These IRFs form the upper force limit for the small female IARBs in this study and are expressed visually in Fig. E2 relative to the original PMHS Knee/Distal Femur IRF. Under force limiting conditions, all ATD load cells are lesser in magnitude than the PMHS applied knee force, so they are to the left of the PMHS IRF.

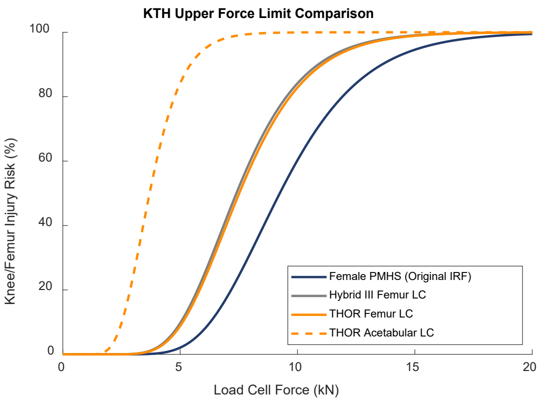

Fig. E2. Comparison of the cadaver-based Knee/Distal Femur IRF used in this study to the ATD IRFs derived using the unique T_{Knee} correction factor for each ATD load cell.

Small Female ATD IARB Values:

TABLE EI

HYBRID III SMALL FEMALE INJURY ASSESSMENT REFERENCE BOUNDARIES (FEMUR LOAD CELL, CURRENT VALUES AND SCALED)

Risk (%)	Lower Force Limit (kN)		Transition Impulse (Ns)		Upper Force Limit (kN)	
Data Source	Female Data	Scaling [8]	Female Data	Scaling [8]	Female Data	Scaling [8]
3	3.41	3.65	57.6	NA*	4.20	3.37
5	3.60	3.82	61.3	NA*	4.50	3.86
10	3.92	4.13	67.8	70.6	5.03	4.66
15	4.15	4.33	72.1	74.1	5.41	5.22
20	4.34	4.49	75.7	77.0	5.74	5.67
25	4.52	4.65	79.1	79.5	6.03	6.06
30	4.68	4.79	82.8	81.9	6.31	6.41
35	4.83	4.91	85.7	84.4	6.58	6.74
40	4.98	5.05	88.3	86.6	6.85	7.04
45	5.14	5.18	92.0	88.9	7.12	7.34
50	5.29	5.33	94.6	91.2	7.40	7.62
75	6.19	6.09	111.8	104.8	9.06	9.14

* Not applicable because the upper and lower-force limits were equal.

TABLE EII

THOR SMALL FEMALE INJURY ASSESSMENT REFERENCE BOUNDARIES (FEMUR AND ACETABULAR LOAD CELLS)

Risk (%)	Lower Force Limit (kN)		Transition Impulse (Ns)		Upper Force Limit (kN)	
Load Cell Location	Femur	Acetabulum	Femur	Acetabulum	Femur	Acetabulum
3	3.46	1.70	46.0	21.3	4.25	2.10
5	3.65	1.80	49.5	23.7	4.56	2.25
10	3.98	1.96	55.7	26.8	5.09	2.51
15	4.21	2.08	60.1	28.8	5.48	2.71
20	4.41	2.17	63.2	30.4	5.81	2.87
25	4.58	2.26	66.4	31.9	6.11	3.02
30	4.75	2.34	68.8	33.2	6.39	3.16
35	4.90	2.42	71.3	34.7	6.67	3.29
40	5.06	2.49	73.8	35.8	6.94	3.43
45	5.21	2.57	76.3	37.1	7.21	3.56
50	5.37	2.64	79.2	38.3	7.49	3.70
75	6.28	3.10	93.8	45.7	9.18	4.53

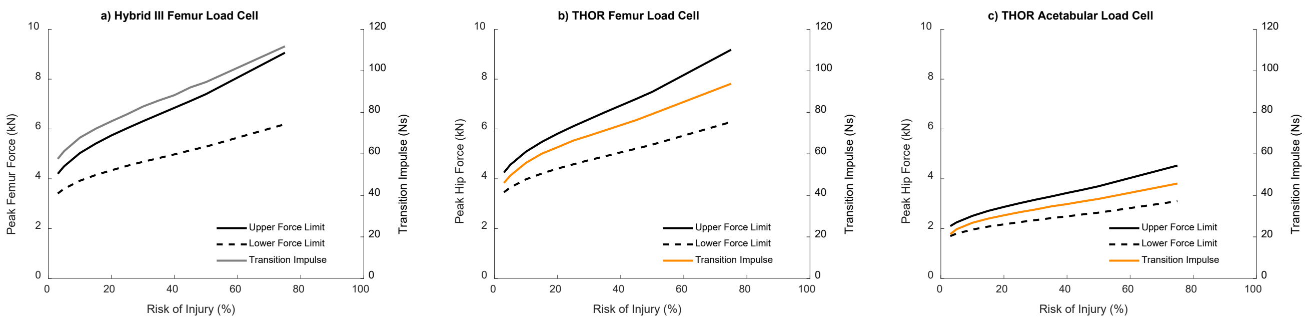

Fig. E3: Final IARB values at various risk levels for each of the small female ATD load cells.

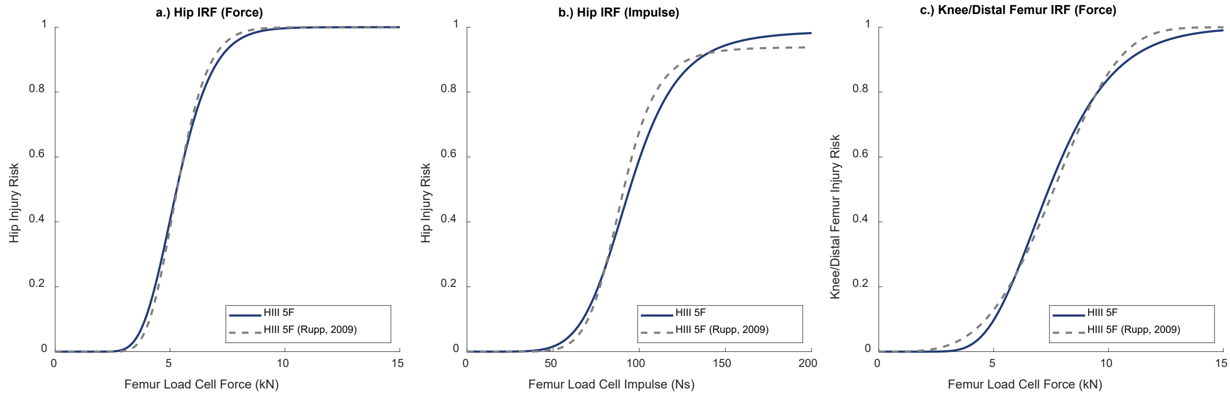

Fig. E4: Comparison of IRFs for the Hybrid III small female (HIII-5F) ATD based on femur load cell measurements, including a.) Hip injury risk as a function of femur load cell force, b.) Hip injury risk as a function of femur load cell impulse, and c.) Knee/distal femur injury risk as a function of femur load cell force. Curves derived from fitted values and IRFs assumed in the current study (solid blue) were compared against reference curves based on scaled midsize male data from [8,31] (dashed grey).

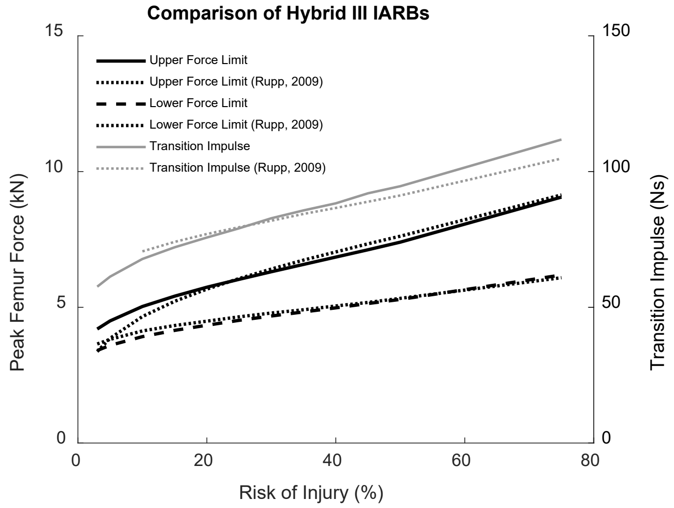

Fig. E5. Comparison of final IARB values at various risk levels for the Hybrid III small female ATD femur load cell. The lower force limit, upper force limit, and transition impulse were compared between the values obtained in the current study, and the ones estimated from scaling the midsize male data in [8].

Scaling the THOR-05F Response to THOR-50M: Since no KTH IARBs currently exist for the THOR-50M, these values were estimated using a combination of methods. To establish the lower and upper force limits for the THOR-50M, the previously discussed IRFs were adapted based on midsize male assumptions (stature = 178 cm, flexion angle = 15°, ♂=1). The correction factors derived for the small female in Table 1 were assumed to be applicable to the midsize male and were applied to the force limits to define the force boundaries. This is assumption is supported by the similarities between the current correction factors derived, and the correction factors estimated in past literature for the THOR-50M [1,39].

Using these assumptions, the upper bound of integration for determining impulse in the THOR-50M femur load cell was calculated as 4.19 kN (i.e., 2.89 kN * (1/0.69)), and for the acetabular load cell as 2.06 kN (i.e., 2.89 kN * (1/1.40)),where 2.89 kN comes directly from [8]. To estimate the corresponding transition impulses, a scaling approach was applied using Equation E18:

$$\lambda_I = \lambda_F * \lambda_t \qquad (E18)$$

Where λ_I is the impulse scaling factor, λ_F is the force scaling factor, and λ_t is the time scaling factor. Previously reported values for the THOR-05F [40] were used, representing the methodology and assumptions utilized to scale the KTH response from the THOR-50M to the THOR-05F. To reverse this scaling (i.e. move from THOR-05F to THOR-50M), the inverse values were applied, yielding an impulse scale factor of approximately 1.47. Applying this correction factor to the impulse values in Table E2, along with the force limits derived from the stated assumptions, resulted in the estimated IARBs for the THOR-50M, as presented in Table E3.

TABLE EIII
ESTIMATED THOR MIDSIZE MALE INJURY ASSESSMENT REFERENCE BOUNDARIES (FEMUR AND ACETABULAR LOAD CELLS)

Risk (%)	Lower Force Limit (kN)		Transition Impulse (Ns) ($\lambda_I = 1.47$)		Upper Force Limit (kN)	
Load Cell Location	Femur	Acetabulum	Femur	Acetabulum	Femur	Acetabulum
3	4.65	2.29	67.6	31.3	6.31	3.12
5	4.91	2.42	72.8	34.8	6.78	3.35
10	5.35	2.64	81.9	39.4	7.56	3.73
15	5.67	2.79	88.3	42.3	8.14	4.02
20	5.93	2.92	92.9	44.7	8.63	4.26
25	6.17	3.04	97.6	46.9	9.08	4.48
30	6.39	3.15	101.1	48.8	9.50	4.69
35	6.60	3.25	104.8	51.0	9.91	4.89
40	6.80	3.35	108.5	52.6	10.31	5.09
45	7.01	3.46	112.2	54.5	10.71	5.29
50	7.22	3.56	116.4	56.3	11.12	5.49
75	8.45	4.17	137.9	67.2	13.63	6.73

Logistic Fit Parameters for Impulse-Based Hip IRFs (Eq. 5):

TABLE EIV
LOGISTIC FIT PARAMETERS FOR IMPULSE-BASED HIP IRFS (EQ. 5)

Subject	*Load Cell Location*	*a*	*b*	*c*
HIII-5F	Femur	0.9891	94.03	6.52
	Femur (Scaled) [8,31]	0.9386	0.58*154.5037	8.7288
THOR-05F	Femur	0.9957	78.73	6.33
	Acetabulum	1.0177	38.52	6.01
THOR-50M	Femur (Scaled)	0.9957	1.47*78.73	6.33
	Acetabulum (Scaled)	1.0177	1.47*38.52	6.01

Appendix F: Example Derivation of KTH Injury Risk Assessment Boundaries Associated with a 25% Risk

Hybrid III Femur Load Cell:

TABLE FI

FORCE HISTORIES USED FOR SMALL FEMALE KTH INJURY ASSESSMENT CRITERIA (25% RISK)

	Force Histories Used to Establish Lower-Force Limit (25% Risk)	*Force Histories Used to Establish Upper-Force Limit (25% Risk)*	*Force Histories Used to Check Transition Impulses (<25% Risk)*
PMHS	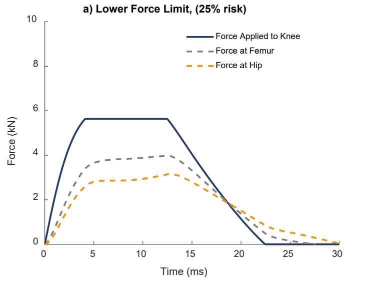	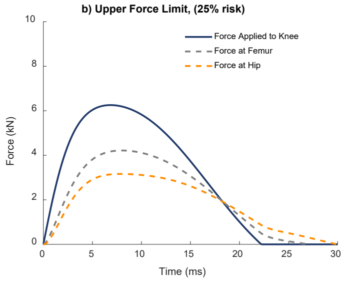	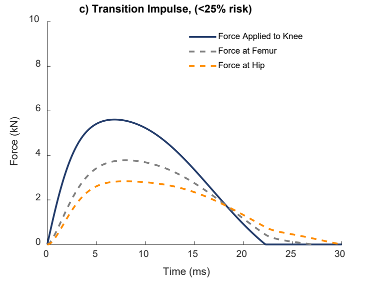
H3 Femur Load Cell	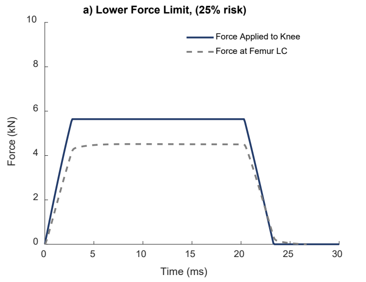	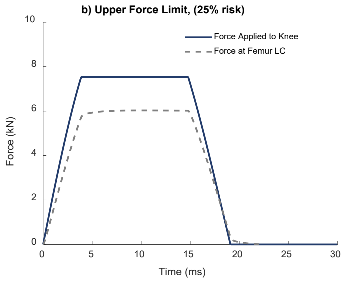	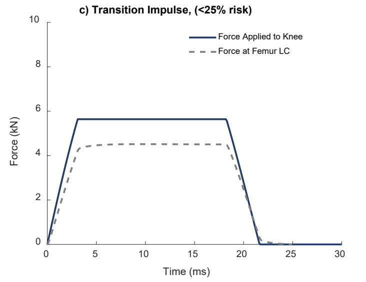
Force Drop	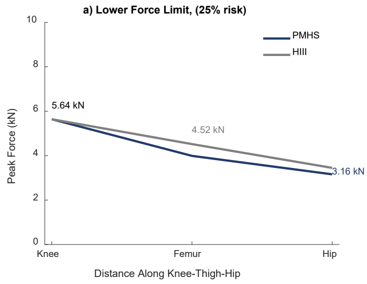	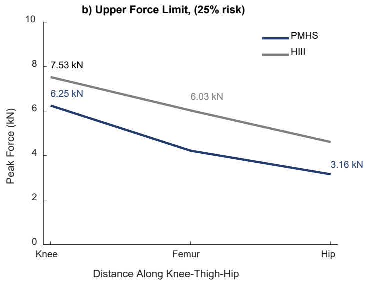	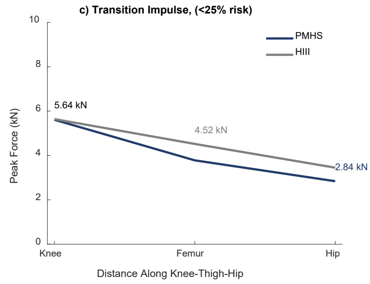
Force-Deflection	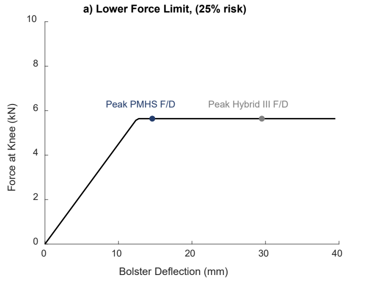	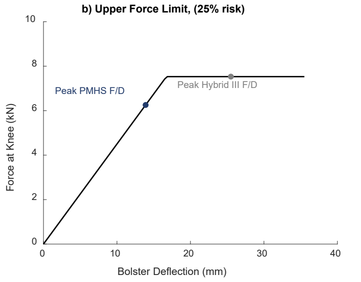	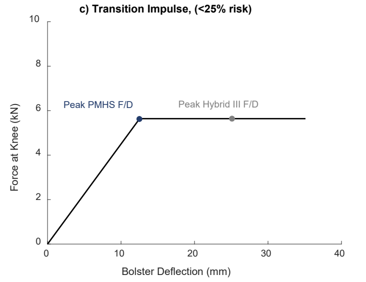

TABLE FII

SIMULATION RESULTS FOR HYBRID III KTH INJURY ASSESSMENT CRITERIA (25% RISK)

Simulation Results		Lower-Force Limit	Upper-Force Limit	Transition Impulse
PMHS Hip Injury Risk		25%	25%	<25%
Impact Velocity		4.88 m/s	4.94 m/s	4.43 m/s
Bolster Stiffness		450,000 N/m	450,000 N/m	450,000 N/m
Force Limit		5.64 kN	7.53 kN	5.64 kN
Bolster Penetration	*PMHS*	14.6 mm	13.9 mm	12.5 mm
	H3	29.5 mm	25.5 mm	25.1 mm
Load Cell Impulse	*Femur*	88.8 Ns	87.8 Ns	79.1 Ns

THOR Femur and Acetabular Load Cells:

TABLE FIII
FORCE HISTORIES USED FOR SMALL FEMALE KTH INJURY ASSESSMENT CRITERIA (25% RISK)

<table>
<tr><th></th><th>Force Histories Used to Establish Lower-Force Limit (25% Risk)</th><th>Force Histories Used to Establish Upper-Force Limit (25% Risk)</th><th>Force Histories Used to Check Transition Impulses (<25% Risk)</th></tr>
<tr><td>PMHS</td><td>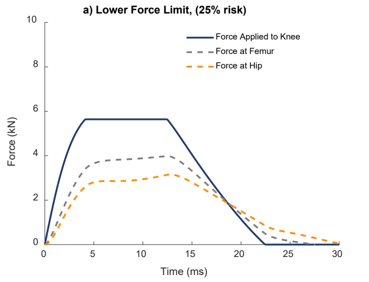
</td><td>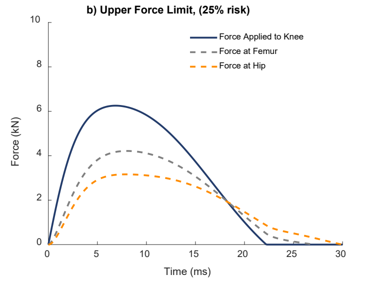
</td><td>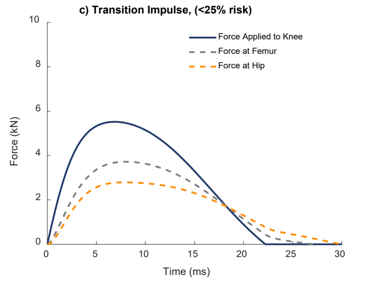
</td></tr>
<tr><td>THOR</td><td>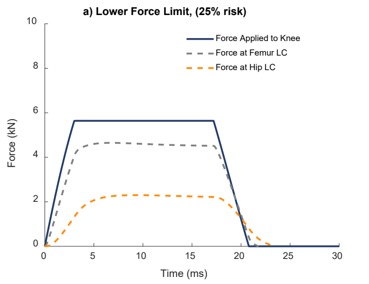
</td><td>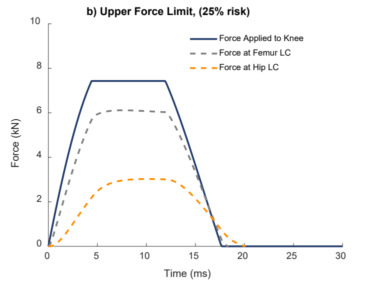
</td><td>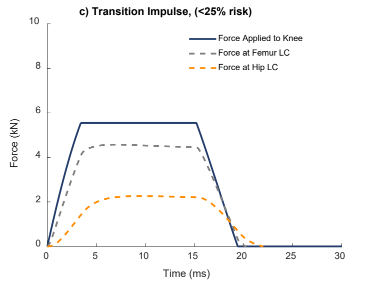
</td></tr>
<tr><td>Force Drop</td><td>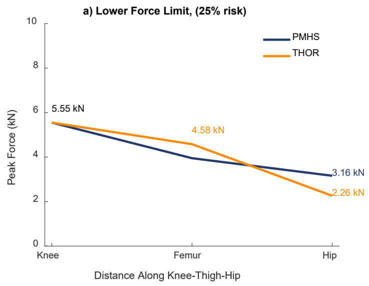
</td><td>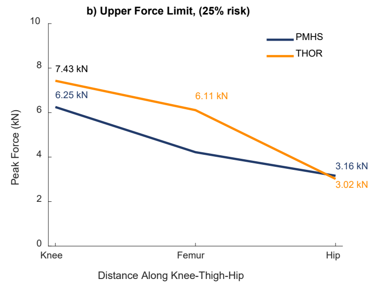
</td><td>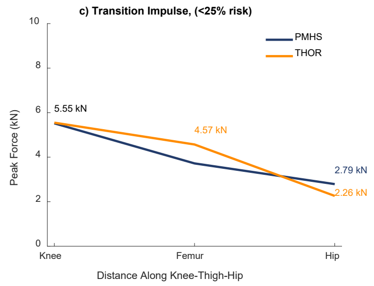
</td></tr>
<tr><td>Force-Deflection</td><td>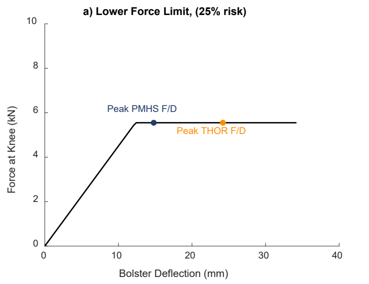
</td><td>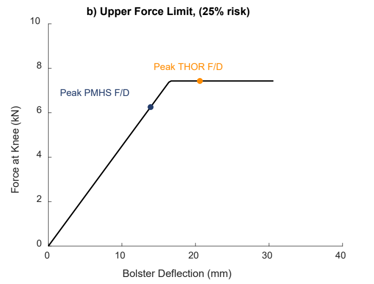
</td><td>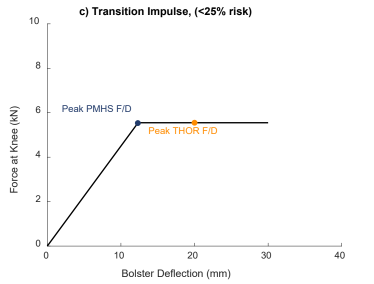
</td></tr>
</table>

TABLE FIV
SIMULATION RESULTS FOR THOR-05F KTH INJURY ASSESSMENT CRITERIA (25% RISK)

Simulation Results		Lower-Force Limit	Upper-Force Limit	Transition Impulse
PMHS Hip Injury Risk		25%	25%	<25%
Impact Velocity		4.87 m/s	4.94 m/s	4.39 m/s
Bolster Stiffness		450,000 N/m	450,000 N/m	450,000 N/m
Force Limit		5.55 kN	7.43 kN	5.55 kN
Bolster Penetration	*PMHS*	14.8 mm	13.9 mm	12.4 mm
	THOR	24.2 mm	20.6 mm	20.2 mm
Load Cell Impulse	*Femur*	76.1 Ns	73.6 Ns	66.4 Ns
	Acetabulum	36.9 Ns	36.0 Ns	32.0 Ns

Appendix G: Evaluation of KTH Injury Assessment Methods Across Data Sources:

Analytical Simulation Data (PMHS):

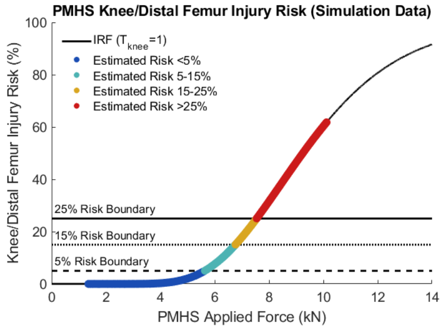

Fig. G1: Estimated PMHS Knee/Distal Femur injury risk across all analytical simulations.

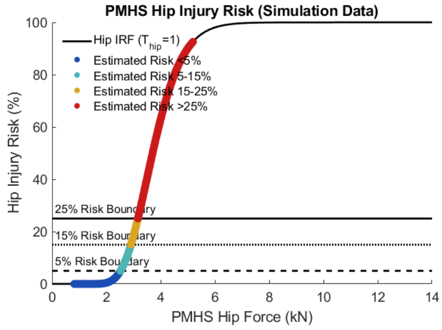

Fig. G2: Estimated PMHS Hip injury risk across all analytical simulations.

TABLE GI
PMHS ESTIMATED KTH INJURY RISK (SIMULATION DATA, N=107,617 SIMULATIONS)

Estimated KTH Injury Risk	Knee/Distal Femur	Hip
<5% Risk (%)	47.17	26.20
5-15% Risk (%)	21.12	12.97
15-25% Risk (%)	13.11	8.10
>25% Risk (%)	18.59	52.73

Analytical Simulation Data (ATDs):

TABLE GII
COMPARISON OF SMALL FEMALE KTH HIP INJURY RISK FROM ANALYTICAL SIMULATIONS (N=107,617 SIMULATIONS PER SUBJECT)

	Conservative Correction Factor Approach Without Impulse	*Experimental Correction Factor Approach*
Hybrid III Femur Load Cell	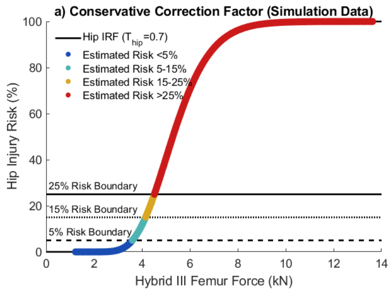	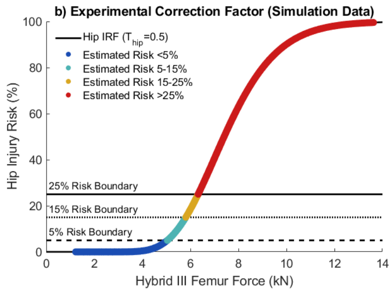
THOR Femur Load Cell	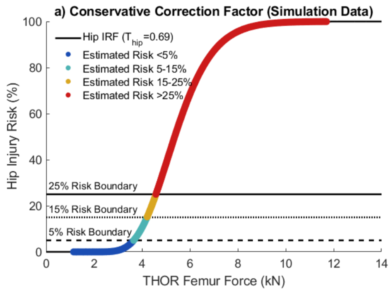	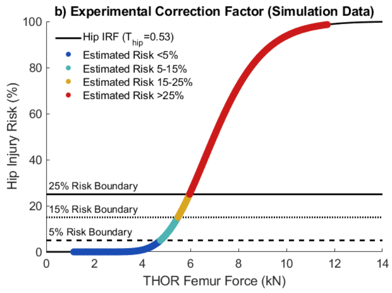
THOR Acetabular Load Cell	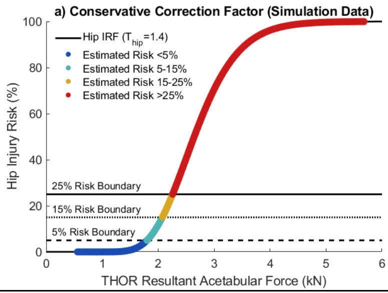	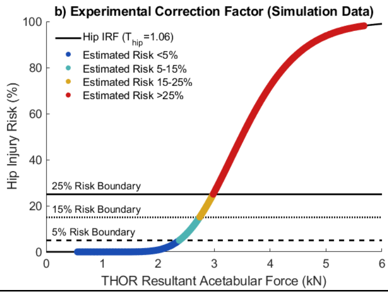

TABLE GIII
FORCE/IMPULSE KTH INJURY ASSESSMENT COMPARISON (SIMULATION DATA, N=107,617 SIMULATIONS PER SUBJECT)

Estimated KTH Injury Risk	Hybrid III Femur	THOR Femur	THOR Acetabulum	Range
<5% Risk (%)	18.05	20.66	20.55	2.61
5-15% Risk (%)	10.45	11.21	11.03	0.76
15-25% Risk (%)	7.15	7.28	7.50	0.35
>25% Risk (%)	64.36	60.85	60.92	3.51

TABLE GIV
CONSERVATIVE CF KTH INJURY ASSESSMENT COMPARISON (SIMULATION DATA, N=107,617 SIMULATIONS PER SUBJECT)

Estimated KTH Injury Risk	Hybrid III Femur	THOR Femur	THOR Acetabulum	Range
<5% Risk (%)	11.75	15.76	15.93	4.18
5-15% Risk (%)	8.44	9.70	9.77	1.33
15-25% Risk (%)	5.61	6.63	6.69	1.08
>25% Risk (%)	74.21	67.91	67.61	6.60

TABLE GV
EXPERIMENTAL CF KTH INJURY ASSESSMENT COMPARISON (SIMULATION DATA, N=107,617 SIMULATIONS PER SUBJECT)

Estimated KTH Injury Risk	Hybrid III Femur	THOR Femur	THOR Acetabulum	Range
<5% Risk (%)	33.91	34.80	36.22	2.31
5-15% Risk (%)	13.30	13.95	14.23	0.93
15-25% Risk (%)	8.72	9.09	9.22	0.50
>25% Risk (%)	44.07	42.16	40.34	3.73

Experimental Knee Impact Data:

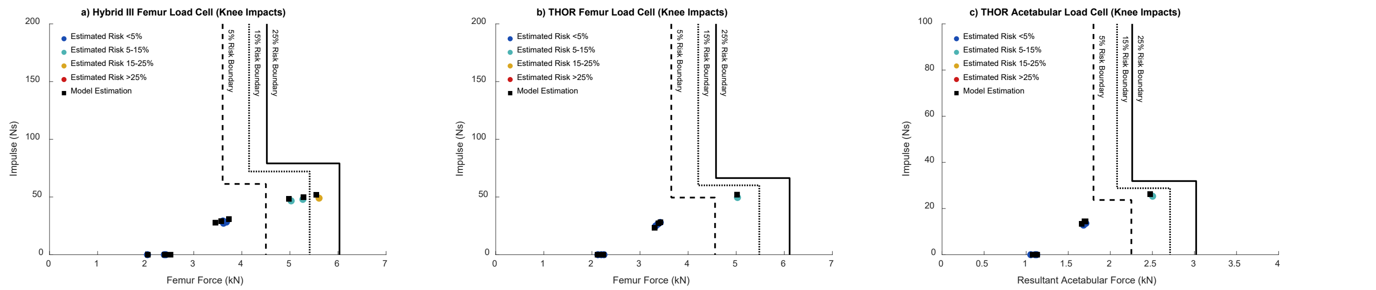

Fig. G3. Comparison of measured and model-estimated load cell forces during the experimental ATD tests [36].

TABLE GVI
COMPARISON OF SMALL FEMALE KTH HIP INJURY RISK FROM EXPERIMENTAL KNEE IMPACTS (N=7-9 TESTS PER SUBJECT)

	Conservative Correction Factor Approach Without Impulse	*Experimental Correction Factor Approach*
Hybrid III Femur Load Cell	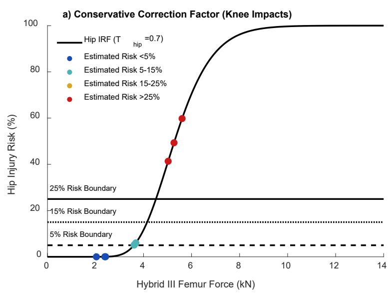	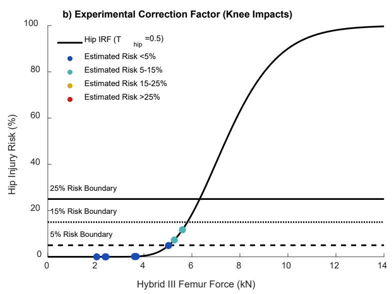

THOR Femur Load Cell

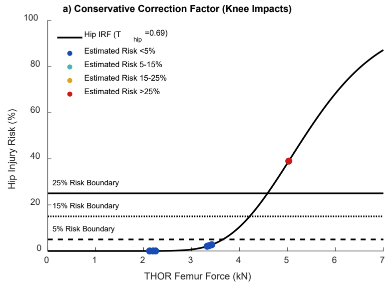

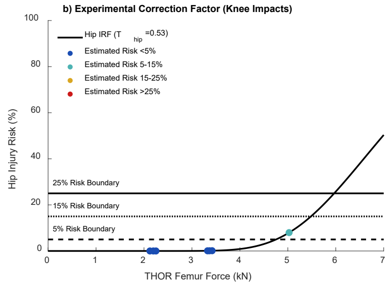

THOR Acetabular Load Cell

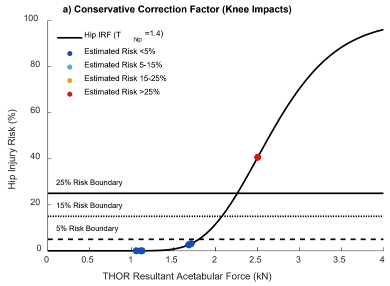

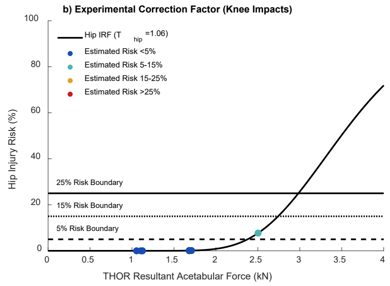

NCAP Passenger Data for Hybrid III Small Female:

TABLE GVII

COMPARISON OF SMALL FEMALE KTH HIP INJURY RISK FROM US NCAP PASSENGER DATA (N=1,130 LOAD CELL MEASUREMENTS)

	Conservative Correction Factor Approach Without Impulse	*Experimental Correction Factor Approach*
Hybrid III Femur Load Cell